High cryptic speciation in the *Pristimantis celator* clade (Anura: Strabomantidae) of the Mira river basin, Ecuador-Colombia (#106009)

First submission

Guidance from your Editor

Please submit by 29 Sep 2024 for the benefit of the authors (and your token reward).



Structure and Criteria

Please read the 'Structure and Criteria' page for guidance.



Custom checks

Make sure you include the custom checks shown below, in your review.



Author notes

Have you read the author notes on the guidance page?



Raw data check

Review the raw data.



Image check

Check that figures and images have not been inappropriately manipulated.

If this article is published your review will be made public. You can choose whether to sign your review. If uploading a PDF please remove any identifiable information (if you want to remain anonymous).

Files

Download and review all files from the <u>materials page</u>.

- 23 Figure file(s)
- 4 Table file(s)
- 1 Raw data file(s)
- 5 Other file(s)



DNA data checks

- Have you checked the authors <u>data deposition statement?</u>
- Can you access the deposited data?
- Has the data been deposited correctly?
- Is the deposition information noted in the manuscript?

Vertebrate animal usage checks

- Have you checked the authors ethical approval statement?
- Were the experiments necessary and ethical?

Have you checked our <u>animal research policies</u>?

New species checks

- Have you checked our <u>new species policies</u>?
- Do you agree that it is a new species?
- Is it correctly described e.g. meets ICZN standard?

For assistance email peer.review@peerj.com

Structure your review

The review form is divided into 5 sections. Please consider these when composing your review:

- 1. BASIC REPORTING
- 2. EXPERIMENTAL DESIGN
- 3. VALIDITY OF THE FINDINGS
- 4. General comments
- 5. Confidential notes to the editor
- You can also annotate this PDF and upload it as part of your review

When ready submit online.

Editorial Criteria

Use these criteria points to structure your review. The full detailed editorial criteria is on your guidance page.

BASIC REPORTING

- Clear, unambiguous, professional English language used throughout.
- Intro & background to show context.
 Literature well referenced & relevant.
- Structure conforms to <u>PeerJ standards</u>, discipline norm, or improved for clarity.
- Figures are relevant, high quality, well labelled & described.
- Raw data supplied (see <u>PeerJ policy</u>).

EXPERIMENTAL DESIGN

- Original primary research within Scope of the journal.
- Research question well defined, relevant & meaningful. It is stated how the research fills an identified knowledge gap.
- Rigorous investigation performed to a high technical & ethical standard.
- Methods described with sufficient detail & information to replicate.

VALIDITY OF THE FINDINGS

- Impact and novelty is not assessed.

 Meaningful replication encouraged where rationale & benefit to literature is clearly stated.
- All underlying data have been provided; they are robust, statistically sound, & controlled.



Conclusions are well stated, linked to original research question & limited to supporting results.

Standout reviewing tips



The best reviewers use these techniques

Τ	p

Support criticisms with evidence from the text or from other sources

Give specific suggestions on how to improve the manuscript

Comment on language and grammar issues

Organize by importance of the issues, and number your points

Please provide constructive criticism, and avoid personal opinions

Comment on strengths (as well as weaknesses) of the manuscript

Example

Smith et al (J of Methodology, 2005, V3, pp 123) have shown that the analysis you use in Lines 241-250 is not the most appropriate for this situation. Please explain why you used this method.

Your introduction needs more detail. I suggest that you improve the description at lines 57-86 to provide more justification for your study (specifically, you should expand upon the knowledge gap being filled).

The English language should be improved to ensure that an international audience can clearly understand your text. Some examples where the language could be improved include lines 23, 77, 121, 128 – the current phrasing makes comprehension difficult. I suggest you have a colleague who is proficient in English and familiar with the subject matter review your manuscript, or contact a professional editing service.

- 1. Your most important issue
- 2. The next most important item
- 3. ...
- 4. The least important points

I thank you for providing the raw data, however your supplemental files need more descriptive metadata identifiers to be useful to future readers. Although your results are compelling, the data analysis should be improved in the following ways: AA, BB, CC

I commend the authors for their extensive data set, compiled over many years of detailed fieldwork. In addition, the manuscript is clearly written in professional, unambiguous language. If there is a weakness, it is in the statistical analysis (as I have noted above) which should be improved upon before Acceptance.



High cryptic speciation in the *Pristimantis celator* clade (Anura: Strabomantidae) of the Mira river basin, Ecuador-Colombia

Mario H Yánez-Muñoz Corresp., 1, Juan P. Reyes-Puig 1, 2, 3, Carolina Reyes-Puig 1, 3, 4, Gabriela Lagla-Chimba 1, Christian Paucar-Veintimilla 1, Miguel A. Urgiles-Merchán 1, Julio C. Carrión-Olmedo 1

Corresponding Author: Mario H Yánez-Muñoz Email address: mayamu@hotmail.com

Over the past decade, research in the montane forests of the Mira River basin, spanning Ecuador and Colombia, has identified it as crucial for the adaptive radiation of flora and fauna, shaped by its complex geological and climatic history. This study focuses on the phylogenetic and systematic revision of a monophyletic frog clade initially labeled as Pristimantis verecundus, revealing significant cryptic diversity. Through detailed analyses of type material and expanded molecular sampling, we identified the original description encompassed three distinct species. Additionally, four new species were discovered within montane forests at elevations from 1600 to 2300 meters. Genetic distances of 3.34% to 14% and clear morphological differences underscore the clade's hidden diversity. We propose renaming the group Pristimantis celator clade within Pristimantis myersi species group and subgenus *Trachyphrynus*, aligning with phylogenetic evidence and resolving taxonomic ambiguities using the oldest available name, Pristimantis celator (Lynch, 1976). This reclassification includes 14 species, seven formally described, and seven as candidates, distributed across northwestern Ecuador and southwestern Colombia, particularly in Mira and Esmeraldas River basins. The study highlights the Andean orogeny's role in species diversification within Pristimantis celator clade, with geographic barriers like Cerro Golondrinas influencing genetic isolation. Genetic divergences exceeding 3.34% indicate evolutionary isolation across these landscapes. Our findings provide insights into montane ecosystem speciation, emphasizing vicariance, niche adaptation, and altitudinal gradients in shaping biodiversity. A polytomy among three wellsupported clades within *Pristimantis myersi* species group is noted due to incomplete genetic data, yet distinctiveness and evolutionary relationships are affirmed. Cryptic

¹ Unidad de Investigación, Instituto Nacional de Biodiversidad (INABIO), Quito, Pichincha, Ecuador

² Red de Bosques Amenazados, Fundación Ecominga, Baños, Tungurahua, Ecuador

Departamento de Ambiente, Fundación Oscar Efren Reyes, Baños, Tungurahua, Ecuador

⁴ Instituto de Biodiversidad Tropical IBIOTROP, Museo de Zoología & Laboratorio de Zoología Terrestres, Colegio de Ciencias Ambientales, Universidad San Francisco de Quito (USFQ), Quito, Pichincha, Ecuador



diversity within *Pristimantis celator* clade links to unique orogenic and climatic conditions, highlighting conservation needs. Lastly, a *Pristimantis verecundus* redescript and species identification key aid future research and conservation in this biogeographically influential region.



1 High cryptic speciation in the *Pristimantis celator*

2 clade (Anura: Strabomantidae) of the Mira river basin,

3 Ecuador-Colombia.

4

- 5 Mario H. Yanez-Muñoz^{1*}, Juan P. Reyes-Puig^{1,2,3}, Carolina Reyes-Puig^{1,3,4}, Gabriela Lagla-
- 6 Chimba¹, Christian Paucar-Veintimilla¹, Miguel Urgiles-Merchan¹ and Julio C. Carrión-Olmedo¹

7

- 8 ¹ Unidad de Investigación, Instituto Nacional de Biodiversidad (INABIO), Quito, Ecuador
- 9 ² Fundación EcoMinga, Red de Protección de Bosques Amenazados, Tungurahua, Ecuador
- 10 ³ Fundación Oscar Efrén Reyes, Departamento de Ambiente, Baños, Ecuador.
- 11 ⁴ Instituto iBIOTROP, Museo de Zoología & Laboratorio de Zoología Terrestre, Colegio de
- 12 Ciencias Biológicas y Ambientales, COCIBA, Universidad San Francisco de Quito USFQ,
- 13 Quito170901, Ecuador.

14

- 15 Corresponding Author:
- 16 Mario H. Yánez-Muñoz¹
- 17 Pasaje Rumipamba 341 y Av. de Los Shyris, Quito-Ecuador.
- 18 Email address: mario.yanez@biodiversidad.gob.ec

19 20

Abstract

- 21 Over the past decade, research in the montane forests of the Mira River basin, spanning Ecuador
- and Colombia, has identified it as crucial for the adaptive radiation of flora and fauna, shaped by
- 23 its complex geological and climatic history. This study focuses on the phylogenetic and
- 24 systematic revision of a monophyletic frog clade initially labeled as *Pristimantis verecundus*,
- 25 revealing significant cryptic diversity. Through detailed analyses of type material and expanded
- 26 molecular sampling, we identified the original description encompassed three distinct species.
- 27 Additionally, four new species were discovered within montane forests at elevations from 1600
- 28 to 2300 meters. Genetic distances of 3.34% to 14% and clear morphological differences
- 29 underscore the clade's hidden diversity. We propose renaming the group *Pristimantis celator*
- 30 clade within *Pristimantis myersi* species group and subgenus *Trachyphrynus*, aligning with
- 31 phylogenetic evidence and resolving taxonomic ambiguities using the oldest available name,
- 32 Pristimantis celator (Lynch, 1976). This reclassification includes 14 species, seven formally
- 33 described, and seven as candidates, distributed across northwestern Ecuador and southwestern
- 34 Colombia, particularly in Mira and Esmeraldas River basins. The study highlights the Andean
- 35 orogeny's role in species diversification within Pristimantis celator clade, with geographic
- 36 barriers like Cerro Golondrinas influencing genetic isolation. Genetic divergences exceeding
- 37 3.34% indicate evolutionary isolation across these landscapes. Our findings provide insights into
- 38 montane ecosystem speciation, emphasizing vicariance, niche adaptation, and altitudinal
- 39 gradients in shaping biodiversity. A polytomy among three well-supported clades within



- 40 Pristimantis myersi species group is noted due to incomplete genetic data, yet distinctiveness and
- 41 evolutionary relationships are affirmed. Cryptic diversity within *Pristimantis celator* clade links
- 42 to unique orogenic and climatic conditions, highlighting conservation needs. Lastly, a
- 43 Pristimantis verecundus redescript and species identification key aid future research and
- 44 conservation in this biogeographically influential region.

Introduction

- 47 The Tropical Andes represent one of the most diverse regions globally in terms of ecosystems,
- 48 habitats, and endemic herpetofauna species. This diversity arises from the region's complex
- 49 geography, geology, elevational, and climate patterns (Duellman, 1979; Lynch & Duellman,
- 50 1997; Pinto-Sánchez et al. 2011; Mendoza et al. 2015; Vasconcelos et al., 2019). In
- 51 northwestern Ecuador, the Mira River drainage cuts through the western cordillera of the Andes,
- 52 forming a deep canyon that connects lowland Chocoan rainforests with high-altitude ecosystems
- 53 in a continuous line. This geographical feature promotes high levels of diversification and
- endemism, particularly within the Mira watershed and its mountain ranges. This pattern is
- evident across several groups of small vertebrates, including amphibians, reptiles, and rodents
- 56 (Yánez-Muñoz *et al.*, 2018, 2021a,b, 2024; Brito Molina *et al.*, 2020; Reyes Puig *et al.*,
- 57 2020a,b).

58

59

60

61

62 63

64

65 66

67

68

69

70 71

72

73

74

75

76

77

78

79

In addition to the broad patterns of diversity across the region, a specific group of mountains located west of Cerro Golondrinas and east of the Awa Indigenous Territories stands out. This area is among the richest in orchids and birds within the Tropical Andes and Chocó regions (Santander, Freile & Loor-Vela, 2009). Notably, it encompasses the Dracula Reserve, which was established to protect key endangered forests and serve as a type locality for newly described batrachians and lizard species (Yánez Muñoz *et al.*, 2018; 2021a,b; Reyes-Puig *et al.*, 2020).

The direct-developing terrestrial frog genus *Pristimantis* Jiménez de la Espada 1890, thrives in the northern Andes of South America, where its unique environment boosts rapid lineage divergence, which continues to increase in this region (Pinto-Sánchez *et al.* 2011; Mendoza *et al.* 2015; Vasconcelos *et al.*, 2019; Yánez-Muñoz *et al.*, 2020; Reyes-Puig & Mancero, 2022). As systematic and phylogenetic studies of the genus deepen, challenges in understanding its diversity and ancestor-descendant relationships are revealed. The *Pristimantis myersi* species group is particularly diverse and cryptic, with high genetic diversity and numerous new nominal species awaiting description (Franco-Mena *et al.*, 2023).

Closely related to this group, *Pristimantis verecundus* (Lynch & Burrowes, 1990) was initially described from a type series with varying coloration patterns, but little is known about the variation in live specimens; a detailed examination of the type material of *Pristimantis verecundus* from Reserva La Planada, revealed contrasting differences between specimens, suggesting that cryptic taxa are blended within the type series. This species has recently shown polyphyletic relationships, suggesting the increase of new taxa, and is currently grouped in the *P. verecundus* clade (Franco-Mena *et al.*, 2023). Over the past decade, we have conducted



systematic expeditions in the extreme northwestern region of Ecuador, which allowed us to collect, examine, and obtain fresh genetic material to better understand this group. In the present work, we increase the phylogenetic sampling of the clade, revealing four new species described here and three additional unnamed species.

Materials & Methods

Ethics statement. This research was conducted under permits granted for access to genetic resources: MAE-DNB-CM-2016-0045, N°MAE-DNB-CM-2019-0120, and MAATE-ARSFC-2023-3346 issued by the Ministry of Environment, Water, and Ecological Transition of Ecuador. The study adhered to guidelines for the use of live amphibians and reptiles in field research (Beaupre *et al.*, 2004) established by the American Society of Ichthyologists and Herpetologists, the Herpetologists' League, and the Society for the Study of Amphibians and Reptiles.

Examined specimens were sourced from the herpetology repositories: Instituto Nacional de Biodiversidad, Quito, Ecuador (DHMECN); Instituto Humboldt, Villa de Leyva, Colombia (IAvH, acronym previously known as IND-AN); and Museo de Zoología Universidad San Francisco de Quito, Quito, Ecuador (ZSFQ). Museum acronyms follow Frost (2024).

Taxon sampling. For the taxonomic descriptions, we used a combination of several lines of evidence, including external morphological characters, linear morphometry variations, genetic divergence, and geographic distribution. We examined high-resolution photographs of the type material of *Pristimantis verecundus* (Lynch & Burrowes, 1990) provided by the IAvH (Supplementary material. Fig.1–2). Similar approaches have been used by us to recognize and identify cryptic amphibian and reptile complexes in the Mira river basin landscape (Yánez-Muñoz *et al.* 2018, 2021a,b, Reyes-Puig *et al.*, 2020a,b).

The electronic version of this article in Portable Document Format (PDF) will represent a published work according to the International Commission on Zoological Nomenclature (ICZN), and hence the new names contained in the electronic version are effectively published under that Code from the electronic edition alone. This published work and the nomenclatural acts it contains have been registered in ZooBank, the online registration system for the ICZN. The ZooBank LSIDs (Life Science Identifiers) can be resolved and the associated information viewed through any standard web browser by appending the LSID to the prefix http://zoobank.org/. The LSID for this publication is: LSIDurn: lsid:zoobank.org:pub:0E31ADC7-D760-427D-A7F6-5E6ADB7A21B5

Field work. Herpetological surveys were steered using visual encounter surveys (Rueda *et al.*

- 115 2006). Field work was conducted in the mountains and tributary drainages of the Mira
- watershed, during expeditions of Instituto Nacional de Biodiversidad (INABIO) and the
- Ecominga Foundation, in 10 locations sampled between the years 2015 to 2023, shown in Table
- 118 1. Like other previous research (Reyes-Puig et al., 2020a,b; Yánez-Muñoz et al., 2021a; Yánez-
- 119 Muñoz et al., 2021b), the specimens collected were photographed alive, euthanized with



benzocaine, a sample of muscle tissue was extracted and preserved in 95% ethanol; the
individuals were fixed in 10% formalin, and preserved in 75% ethanol, as referred in Rueda *et al.*2006.

123124

125

126

127

128129

130

131132

133

134

135

136

137

138

139

140141

142

143

144

145146

147

148

149150

151

152

Morphological data. The taxonomic terminology follows the proposal of Duellman and Lehr (2009). Morphometric measurements were taken with an electronic caliper (accuracy ± 0.01 mm, rounded to 0.1 mm). The following morphological measurements were taken following similar descriptions (Duellman & Lehr, 2009; Reyes-Puig et al., 2020b): (1) snout-vent length (SVL) = distance from snout tip to posterior margin of vent; (2) head width (HW) = greatest width of head measured at level of jaw articulation; (3) head length (HL) = from posterior margin of lower jaw to tip of snout; (4) horizontal eve diameter (ED) = distance between anterior and posterior borders of eye; (5) interorbital distance (IOD) = the breadth of the braincase between the orbits; (6) eye–nostril distance (EN) = distance from posterior margin of nostril to anterior margin of eye; (7) tympanic length (TD) = horizontal distance between external anterior and posterior margins of tympanic annulus; (8) internarinal distance (IND) = from the external border of nostrils; (9) tibia length (TL) = length of flexed leg from knee to heel; (10) upper evelid width (EW) = perpendicular distance of the upper evelid; (11) foot length (FoL) = distance from the proximal edge of the medial metatarsal tubercle to the tip of the fourth toe; (12) hand length (HaL) = distance from proximal edge of palmar tubercle to tip of Finger III; (13) disc width of finger III (F3D) = measured across widest part of finger disc III: (14) disc width of toe IV (T4D) = measured across widest part of toe disc IV. Fingers are numbered preaxially to post-axially from I-IV. Comparative lengths of toes III and V were determined, both compared to toe IV; lengths of toes I and II were estimated compared to each other. Sex, maturity of specimens, and reproductive condition were delimited by the identification of vocal slits, size, and through direct observation of gonads by dorsolateral sectioning.

Sexual dimorphism was analyzed descriptively by visualizing the variation in body size (SVL) between sexes using box plots (Supplementary material Fig.3). The analysis was conducted using the statistical package Past [®] (Hammer, Harper & Ryan, 2001).

To minimize phenotypic plasticity within the clade (Guayasamin *et al.* 2015), only those characters that were documented and preserved 12 hours after collection, were considered diagnostic. Color in life was determined based on photographs taken in the field from original collectors. In the descriptive section of living and preserved colorations of the type series of the new species, the colors are accompanied by the catalog number associated with the Köhler (2012) standard in parentheses.

153154155

156

157

158159

DNA extraction, amplification, sequencing, and bioinformatics. DNA extraction and PCR amplification followed the methodology described in Reyes-Puig *et al.* (2024). Partial mitogenomes were amplified, flanking 12S rRNA to ND1 region. Three contiguous mitochondrial genes 12S rRNA, 16S rRNA, and NADH dehydrogenase subunit 1 (ND1) were amplified. We targeted two overlapping >2000bp mitochondrial fragments using a mid-range



170

171

172173

180

181 182

183

184

185 186

187

188

189 190

191

192

193194

195

196

197198

- PCR to amplify multiple genes at once. The first fragment flanks from 12S to 16S using 12sL4E
- 161 (TACACATGCAAGTYTCCGC) with 16H36E (AAGCTCCAWAGGGTCTTCTCGTC)
- 162 (Heinicke et al. 2007), with the following thermocycler protocol: 5 min @ 95 °C, then 35 cycles
- of: 45 secs at 95 °C, 35 secs at 50°C, and 2 min at 72°C, then 5 min at 72°C. The second
- 164 fragment flanks 16S-ND1 using 16L19 (AATACCTAACGAACTTAGCGATAGCTGGTT)
- with t-Met-frog (TTGGGGTATGGGCCCAAAAGCT) (Wiens et al. 2005, Moen and Wiens
- 166 2009), with the following thermocycler protocol: initial denaturation 5 min @ 95°C, 30 secs at
- 167 95 °C, 30 secs at 57 °C and 4 min at 72 °C for 35 cycles, with a final extension time of 5 min at 168 72 °C.

Chosen molecular markers (12S rRNA, 16S rRNA, and ND1) are widely used in amphibian phylogenetics (Hay *et al.* 1995, Chan *et al.* 2022, Portik *et al.* 2023).

Sequencing run was performed on a minION mk1c using Flongle Flow Cells R10.4.1 and Rapid Barcoding Kit 96 V14 (SQK-RBK114.96) following manufacturer protocols. Raw reads were high-accuracy (HAC) basecalled and demultiplexed with Dorado 7.3.11.

174 Consensus sequences were generated with NGSpeciesID (Sahlin et al. 2021) using above Q12

- fastq reads. Consensus sequences expected divergence from Sanger between 0.00-0.04%
- 176 (Vasiljevic et al., 2021), too small to be consequential to robust phylogenetic analysis. FASTQ
- 177 files management, consensus generation, and subsequent FASTA files management, renaming,
- and concatenation were automated using a custom Python script available in Zenodo by Carrión-Olmedo (2024).

DNA extraction, PCR amplification, nanopore sequencing, and bioinformatic analysis were performed at the Nucleic Acid Sequencing Laboratory of the Instituto Nacional de Biodiversidad (INABIO) in Quito, Ecuador. 67 consensus sequences were generated (20 of 12S, 29 of 16S, and 18 of ND1) of 29 individuals. Generated sequences were imported and interpreted using Mesquite (Maddison and Maddison 2018).

The newly generated sequences are available in GenBank (Supplemental material 1) as suggested by Chakrabarty *et al.* (2013). We expanded our study group to include species shown to be closely related to *Pristimantis verecundus* based on Franco-Mena *et al.* (2023) and an unpublished phylogeny of *Pristimantis* obtained by Julio C. Carrión-Olmedo as part of a large-scale review of northern *Pristimantis*.

Due to genetic data availability, we first constructed a 16S matrix to infer the phylogenetic position among congeners based on the phylogeny of Franco-Mena *et al.* (2023). To infer a more robust phylogenetic placements of new lineages within the scope of this group we constructed a partitioned matrix with the partial mitogenomes from 12S rRNA to ND1. Matrices were aligned using default parameters in MAFFT (Katoh & Standley, 2013) and visually inspected for unambiguous alignment errors.

Substitution models and maximum likelihood tree inference were performed using IQ-TREE (Trifinopoulos *et al.* 2016) under default settings. Branch support was evaluated using 2000 ultrafast bootstrapping and SH-aLRT tests with 1000 replicates (Guindon *et al.* 2010).



199 Uncorrected p-distances were calculated with an 800 bp-long fragment of 16S rRNA using 200 MEGA 11(Tamura *et al.*, 2021).

Results

Phylogenetic relationships and genetic distances (Fig. 1). The 16S exploratory matrix was 1653 bp long for 330 individuals and the partial mitogenomes matrix was 3958 bp long for 99 individuals. IQTree evaluated the best substitution model for 8 partitions as follows: TIM2+F+G4 for 12S rRNA, TIM2+F+I+G4 for 16S rRNA, TIM2e+G4 for ND1 first position,

TPM3+F+G4 for ND1 second position, TIM+F+G4 for ND1 third position.

The positioning of the study clade and species in the genus *Pristimantis* was highly supported (Fig. 1A). We expand the phylogenetic diversity knowledge and the number of species on the *Pristimantis verecundus* clade *sensu* Franco-Mena *et al.* (2023), from 10 to 14 species (Fig. 1A). Like Franco-Mena *et al.* (2023), we also identified the unresolved evolutionary relationships among the *Pristimantis myersi* species group (Fig 1B.). Three well-supported clades formed a polytomy, the first clade (90.7/100 branch supports) is composed by *Pristimantis celator+P. mutabilis+P. verecundus* and several candidate species, the second clade (57.7/93 branch supports) is composed of *P. jubatus+P.* c.sp. 1, and the last clade is the *P. myersi* clade (79/96 branch supports).

An undescribed species from the clade of *Pristimantis verecundus* reported as *P.* sp. 3 from Via Ibarra-San Lorenzo by Franco-Mena *et al.* (2023) is here described as *P. praemortuus* sp. nov. and it is sister species of *P. broaddus* sp. nov. (97.1/100 branch supports). Similarly, *Pristimantis* sp. 5 reported by Franco-Mena *et al.* (2023) is here described as *P. satheri* sp. nov.. Additionally, as we increased the sampling, a new unreported lineage was included within the *Pristimantis verecundus* clade, here we describe it as *P. robayoi* sp.nov., a closely related species to *P. verecundus* (Lynch & Burrowes, 1990).

Franco-Mena et al. (2023) in nominating the Pristimantis verecundus clade, did not consider taxonomically that Pristimantis celator (Lynch, 1976) is the oldest available name for the clade. Formally, we define the Pristimantis verecundus clade (sensu Franco-Mena Mena et al. 2023) nominally as the Pristimantis celator clade. We consider that despite the polytomy confirmed in this and other research (Franco-Mena et al. 2023), the Pristimantis jubatus clade and Pristimantis celator clade should be part of the Pristimantis myersi species group, into the subgenus Trachyphrynus (Hedges et al., 2008; Rivera-Correa & Daza 2016; Gonzalez et al., 2018; Rivera et al., 2017; Jetz & Pyron 2018; Bejarano et al., 2022).

Pristimantis celator clade (Fig 1A.) is composed of two subclades. The subclade A has high support (99.9/100) for grouping one candidate species (*P*. sp.1) and two new sister species described herein (*P. broaddus* sp. nov.+*P. praemortuus* sp. nov.). Previously, Franco-Mena *et al.* (2023) identified *Pristimantis* sp.1 (in our phylogeny) as *P.* sp.2. The subclade B has a medium support (54.9/92) and contains a subclade of moderately high support (82.4/100) formed by *Pristimantis satheri* sp. nov.+one candidate species (*P.* sp. 2, reported as *P.* sp. 4 by Franco-Mena *et al.* 2023). Which is a sister of a high support subclade (97.4/100) comprised of *P.*



- 239 celator, P. mutabilis, five new candidate species (in our phylogeny P. sp. 3, P. sp.4, P. sp.5, P.
- sp.6, P. sp.7 reported by Franco-Mena et al. 2023 as P. sp. 6, P. sp. 7, P. sp. 8, P. sp. 10, and P. 240
- 241 sp. 9 respectively), and *Pristimantis verecundus* with its closely related species *Pristimantis*
- 242 robayoi sp. nov.

- Systematic accounts
- Pristimantis (Trachyphrynus) celator clade 245
- **Definition.** Small-sized frogs with proportionally long limbs; ecotypes slender-bodied terrestrial 246
- and bush frogs; SVL in males ranges from 12.46 mm in males of *Pristimantis praemortuus* 247
- sp.nov. to 29.5 mm in females *P. robayoi* sp. nov. Dorsolateral dermal or glandular folds present 248
- (except in *Pristimantis celator*). Head width 33.76–39.6% of SVL. The tympanic membrane and 249
- 250 annulus are distinctive or partially concealed beneath thin skin on side of head. Dorsum finely
- shagreen to tuberculate, venter areolate, with rounded small tubercles; tubercles subconical or 251
- 252 conical in the upper the eyelid and hells. Interdigital membranes absent and the Toe V is much
- 253
- longer than the Toe III. Tip of Toe V reaching distal border of distal subarticular tubercle of toe
- IV (Condition C). Fingers with lateral fringes or crenulations; Toes with lateral fringes or keels. 254
- Vocal slits and nuptial pads present or absent. 255

256

- 257 **Diversity** (Fig. 2). Fourteen species, seven formally described: *Pristimantis celator* (Lynch,
- 1976), Pristimantis verecundus (Lynch & Burrowes, 1990), Pristimantis mutabilis (Guayasamin 258
- et al., 2015), Pristimantis broaddus sp. nov., Pristimantis praemortuus sp. nov., Pristimantis 259
- robayoi sp. nov., Pristimantis satheri sp. nov., and seven candidate species 1 (P. csp.1–P. csp.7, 260
- 261 Fig. 1–2).

262

- **Distribution** (Fig. 3). Restricted to the Andean montane forest slopes of northwestern Ecuador 263
- (Carchi, Imbabura, Pichincha, and Cotopaxi provinces) and southwestern Colombia (Nariño 264
- 265 Department), between the Esmeraldas and Mira river basins, at elevation ranges from 500 m to
- 2200 m elevation. Inhabit in Western foothill forest, Western Low Montane Forest, and Western 266
- 267 montane forest ecosystems (MAE 2013).

- 269 Comments. Originally Hedges et al. (2008) determined the phylogenetic position of Pristimantis
- 270 verecundus from material collected in Cotopaxi province (QCAZ 12410) assigning it to the P.
- 271 unistrigatus species group. Based on this published sequence, Padial et al. (2014) do not include
- 272 it in any species group. Franco-Mena et al. (2023) identify the Pristimantis verecundus clade in
- 273 polytomy with the *Pristimantis myersi* group, although, Guayasamin et al. (2019) previously
- reported the monophyly of these clades.. It also determines that the sequence used by Hedges et 274
- 275 al. (2008) and Padial et al. (2014) corresponds to a new candidate species, assigns sensu stricto
- sequences of *Pristimantis verecundus*, and determines high cryptic diversity. In this work, we 276
- reorganize the Pristimantis verecundus clade redefined it as the Pristimantis celator clade, and 277
- 278 assign this clade as part of the *Pristimantis myersi* species group. We consider the polytomy



- between the *Pristimantis jubatus+P. celator* clades with the *Pristimantis myersi* group are due to
- 280 the small size of the available sequences of *Pristimantis jubatus*. We confirm the close
- 281 relationship between the *Pristimantis myersi* species group and the *Pristimantis*
- 282 leptlophus+P.boulengeri+ P. devillei groups, therefore, like other authors, we suggest that this
- 283 large, high-support clade should be considered the subgenus *Trachyphrynus* (Hedges *et al.*,
- 284 2008; Rivera-Correa & Daza 2016; Gonzalez et al., 2017; Rivera et al., 2017; Jetz & Pyron
- 285 2018; Bejarano et al., 2022).
- 287 New species
- 288 Pristimantis praemortuus sp. nov.
- 289 Pristimantis sp.5 Franco-Mena et al. 2023.
- 290 LSIDurn: lsid:zoobank.org:act:0C3E9CF7-3D61-4440-8203-C3E4A5D582C0
- 291 Common name in Spanish: Cutín de Praemortuus
- 292 Suggested common English name: Praemortuus's rainfrog
- 293

- 294 **Holotype** (Figs. 2, 4–9). DHMECN 19591, adult female, from the Bloque 20, Sector Los Olivos
- 295 (Bloque 20), Dracula Reserve, Tulcán, Carchi province, Ecuador, (0.84349, -78.21272; 2339 m),
- 296 collected on 13 December 2023 by Mario Humberto Yánez-Muñoz, Christian Paucar
- 297 Veintimilla, Carlos Ríos & Miguel Urgilés-Merchán.
- 298
- 299 Paratype (Supplementary material Fig.4). A total of seven specimens were collected in the same
- 300 type locality and data collectors. Adult females (2): DHMECN 19557 and DHMECN 19570
- 301 (0.83239, -78.24377; 2390 m) on 08 December 2023. Adult males (3): DHMECN 19535
- 302 (0.83829, -78.22830; 2379 m); DHMECN 19546 and DHMECN 19547, (0.83572, -78.23136;
- 303 2288 m) DHMECN 19577, (0.83989, -78.22341; 2357 m); collected on 08 December 2023 and
- one juvenile DHMECN 19579, (0.84025, -78.22314; 2351 m), collected on 12 December 2023.
- 305
- 306 **Diagnosis.** Pristimantis praemortuus sp. nov. is a member of the Pristimantis myersi species
- group and *P. celator* species clade, characterized by the following combination of characters: (1)
- dorsal skin shagreen with scattered low tubercles throughout the body; flanks with subconical
- 309 tubercles aggregated in the axillary region; small subconical tubercles on the ventral edge of the
- 310 lower jaw; dorsolateral fold present well-defined, extending from the scapular region to or
- 311 slightly beyond the sacral region (illium), the dorsal surface of the tibia covered by transverse
- 312 rows of glandular tissue, discoidal fold present slightly visible, venter areolate with tiny
- 313 scattered tubercles; (2) tympanum present, visible, tympanic annulus clearly defined, round,
- 314 posterior border of tympanic annulus with a thick fold, horizontal diameter of tympanum equal
- 315 to 49.5% of eye diameter, antero-dorsal margin with a supratympanic fold composed by low
- warts, subconical postrictal tubercles present; (3) snout short, broadly rounded in dorsal view,
- short, curved, tip of snout protruding in lateral view; (4) upper eyelid with one small conical
- 318 tubercle and with several lower subconical tubercles; cranial crest absent; (5) dentigerous
- 319 processes of vomers positioned posterior to level of choanae, obliques in posterior outline,



321

322

323 324

325

326

327

328 329

330

331 332

333

334 335 minute and embedded inf roof of mouth, barely visible and therefore sometimes considered to be absent; (6) males unknown; (7) finger I shorter than finger II; discs broad and expanded mainly in the fingers II-IV, with circummarginal grooves; (8) fingers with lateral fringes, weakly defined; (9) ulnar tubercles present, subconical placed on the outer edge of the ulna; (10) heel with an elongated conical tubercle surrounded by lower rounded tubercles, outer edge of the tarsus with a row of subconical tubercles, internal tarsal fold weakly defined; (11) metatarsal tubercle 2X larger than the external one which is rounded and subconical; few supernumerary tubercles and barely visible; (12) toes with weakly defined lateral fringes, basally pronounced, interdigital membrane absent, outer edge of the foot and toe IV crenulated, toe V longer than toe III, does not reach the base of the distal subarticular tubercle of the toe IV; (13) Dorsal color pattern grayish olive to with jet black (300) (chestnut to maroon in life), ventrally marmoleated with jet black to medium neutral gray with an inverted trapezoidal mark (throat with a distinctive incomplete trapezoidal burn umber in life). Hidden surfaces of thighs, legs, and groin are pinkish in preservative (reddish in life). Iris coppery gold to copper; (14) small adult males, SVL= 12.46-16.09 mm (mean = 14.28 mm, n= 4), females SVL= 17.03-17.68 mm (mean = 17.35 mm, n= 3).

Comparison with other species (Fig. 2, 6–8). The new species and its closest sister species 336 (Pristimantis broaddus sp. nov.) are the only species on the P. celator clade in having narrow 337 digits of toes. P. paermortuus sp. nov. differs from the closely related species (P. verecundus, P. 338 mutabilis, P. robayoi sp. nov., P. satheri sp. nov., and P. broaddus sp. nov., Fig. 1) by the 339 presence of dorsolateral fold well-defined visible from the scapular region to or slightly beyond 340 the sacral region (ilium) (complete dorsolateral glandular folds extending to the first quarter of 341 342 the ilium in P. satheri sp. nov, dorsolateral fold reaching just before the sacrum in P. verecundus, dorsolateral fold only reach the level of sacrum in *P. mutabilis*, dorsolateral folds extending the 343

entire length of the ilium in P. robayoi sp. nov); throat with an inverted trapezoidal mark (V-344 shaped mark in P. verecundus, reduced or inconspicuous in P. mutabilis and absent in P. robayoi 345 346 sp. nov and P. satheri sp. nov); the dorsal surface of the tibia covered by transverse rows of glandular tissue in P. broaddus sp. nov, P. verecundus and P. praemortuus sp. nov (outlining the 347 extreme edge of the heel in P. robayoi sp. nov, dorsal surface of tibia covered by glandular tissue 348 in P. satheri sp. nov); and iris gold red in P. broaddus sp. nov (bright orange-copper with a 349 350 black edge in P. robayoi sp. nov., coppery gold in P. praemortuus, sp. nov iris cream to golden with thin black reticulation and a reddish-brown horizontal streak in P. mutabilis, and wine-351 352 colored in P. satheri sp. nov). Tympanic annulus clearly defined, round, posterior border of tympanic annulus with a thick fold in *P. praemortuus* sp. nov (tympanic annulus weekly defined 353 in P. broaddus sp. nov), fingers with lateral fringes weakly defined in P. praemortuus sp. nov 354

(strongly crenulated mainly in finger IV lateral fringes in *P. broaddus*), toes with weakly defined lateral fringes, basally pronounced, interdigital membrane absent, outer edge of the foot and toe

357 IV crenulated in *P. praemortuus* sp. nov (toes with weakly defined lateral fringes, basally

pronounced, interdigital membrane absent in *P. broaddus*).



Genetic distances with close-related species (*Pristimantis praemortuus* sp. nov. vs. *P. broaddus* sp. nov.) have 3.54%. The genetic distances with other species in this clade range from 3.54%–12.49% (Supplementary Table 1)

361 362 363

364

365

366

367

368

369

370 371

372

373

374

375376

377

378379

380 381

382

383

384 385

386

387

388 389

390

391

392

393 394

359

360

Description of the holotype (Figs. 4, 9). Adult female (DHMECN 19591), head slightly wider than long. Snout short, broadly rounded in dorsal view, short, curved, tip of snout protruding in lateral view with low rounded scattered tubercles; eye-nostril distance 9.44% of SVL, canthus rostralis slighthly rounded in cross section, in dorsal view weakly concave, loreal region concave, slightly protruding narines directed dorsolaterally; interorbital area with a low rounded interorbital tubercule, interorbital fold absent, interorbital distance wider than upper evelid, 81.42%; cranial crest absent, low dermal fold in the occipital and prootic region; upper evelid with one small conical tubercle and with several lower subconical tubercles (reduced by preservation effects); cranial crest absent, tympanum present, visible, tympanic annulus clearly defined, round, posterior border of tympanic annulus with a thick fold, horizontal diameter of tympanum equal to 49.5% of eye diameter, antero-dorsal margin with a supratympanic fold composed by low warts, subconical postrictal tubercles present, diameter of tympanum equals 45.83% of eye diameter, underside of tympanum with large 2 or 3 subconical postrictal tubercles, subconical; choanae small, oval in outline, not covered by palatal floor of maxilla; dentigerous processes of vomers positioned posterior to level of choanae, obliques in posterior outline, minute and embedded inf roof of mouth, barely visible, no visible teeth, tongue as wide as long, oval, 40% attached to floor of mouth.

Texture of dorsum shagreen with scattered low tubercles throughout the body; flanks with subconical tubercles aggregated in the axillary region; small subconical tubercles on the ventral edge of the lower jaw; dorsolateral fold present well-defined, extending from the scapular region to or slightly beyond the sacral region (ilium), discoidal fold present slightly visible, venter areolate with tiny scattered tubercles; two evident ulnar tubercles present, subconical placed on the outer edge of the ulna; outer palmar tubercle lobular, segmented into three parts, approximately two times the size of elongated outer thenar tubercle; supernumerary tubercles present; subarticular tubercles defined, rounded in lateral view. Fingers with lateral fringes, weakly defined, discs about 1.8× the size of the digit. Hind limbs slender (TL 45.47% of SVL; FL 48.99% of SVL); heel with an elongated conical tubercle surrounded by lower rounded tubercles, outer edge of the tarsus with a row of subconical tubercles, internal tarsal fold weakly defined; metatarsal tubercle larger than the external one which is rounded and subconical; few barely visible supernumerary tubercles; toes have weakly defined lateral fringes that are more pronounced at the base, lack an interdigital membrane, and exhibit crenulation along the outer edge of the foot and toe IV. Toe V is longer than toe III but does not extend to the base of the distal subarticular tubercle of toe IV.

395 396 397

398

Holotype coloration in preservative (Fig. 4). Dorsum grayish olive (274) with scattered irregular yellowish-green marks and distinctive grayish olive (274) stripes on the flanks bordered



in cream, with orange-cream dorsolateral folds. Limbs have grayish olive (274) transverse bands separated by creamy white interspaces. Venter creamy gray marbled with grayish brown (284), with a distinctive grayish brown (284) trapezoidal mark and other irregular grayish brown (284) marks on the throat.

Holotype coloration in life (Fig. 9). Dorsal coloration chestnut (30), with distinctive cinnamon (21) diagonal stripes on the flanks, bordered with cream. Dorsolateral folds burnt umber (48). Chestnut (30) supratympanic stripe, solid and complete, reaching the postrictal tubercle, with cream anterior border. Labial stripes and transversal tibial (glandular) folds chestnut (30). Outer heel edge leaf green (122). Iris copper. Ventrally robin rufous (29), mottled with burnt umber (48), with scattered burnt umber (48) tubercles, throat with a distinctive trapezoidal burnt umber (48) mark.

Measurements (in mm) of holotype. SVL = 17.68; HW = 6.22; HL = 5.37; ED = 2.4; IOD = 1.83; EN = 1.67; TD = 1.1; IND = 1.79; TL = 8.67; EW = 1.49; FoL = 9.02; HaL = 5.36; FW = 0.88; TW = 0.61.

 Variation. *Pristimantis praemortuus* sp. nov. shows sexual dimorphism in body size (Supplementary Fig. 3) and coloration (Fig. 6; Supplementary Fig. 4). Males of this species between 0.6–0.8 times smaller in SVL than females (Fig. supp.3). Other morphometric variation in the type series is showing in the Table 2.

In life (Fig. 6), dorsal coloration chestnut (30) (DHMECN 19535, DHMECN 19547, DHMECN 19546, DHMECN 19591) to maroon (39) (DHMECN 19557, DHMECN 19570), with distinctive diagonal stripes on the flanks ranging from cinnamon (21) (DHMECN 19535, DHMECN 19547, DHMECN 19546, DHMECN 19591) to burnt sienna (DHMECN 19557, DHMECN 19570), bordered in cream. The dorsum may display speckled marks of leaf green (122) (DHMECN 19535, DHMECN 19570), dorsolateral folds reddish-brown (DHMECN 19557, DHMECN 19557) to carmine (64) (DHMECN 19546, DHMECN 19591), burnt umber (48) (DHMECN 19570), or ferruginous (35) (DHMECN 19557). Chestnut (30) supratympanic stripe, solid and complete, reaching the postrictal tubercle, with cream anterior border. Labial stripes and transversal tibial (glandular) folds chestnut (30). Outer heel edge leaf green (DHMECN 19546, DHMECN 19591, DHMECN 19570, DHMECN 19557). Iris coppery gold to copper. Ventrally robin rufous (29) (DHMECN 19546, DHMECN 19557) to burnt sienna (38) (DHMECN 19591, DHMECN 19570), speckled or mottled with burnt umber (48), with scattered burnt umber (48) or reddish-brown tubercles (DHMECN 19546), throat with a distinctive incomplete trapezoidal burn umber (48).

In preservative (Supplementary Fig. 4), dorsal color pattern varies from grayish olive (274) (DHMECN 19591, 19547, 19538), medium neutral grey (299) (DHMECN 19547) to with jet black (300) (DHMECN 19535). Limbs coloration with oblique bars sepia (286) (DHMECN 19547) or army brown (46) (DHMECN 19546). Belly marmoleated with jet black (300), to



- 439 medium neutral gray (298) (DHMECN 19591, 19546–47) to pale neutral gray (296) (DHMECN
- 440 19535, 19570) background. Colorations salmon (251) (DHMECN 19577) to pale neutral gray
- 441 (12) (DHMECN 19535, 19570 19546) on the groins and thigs and metatarsal regions, fingers and
- 442 toes.

Etymology. From the Latin "*praemortuus*", meaning: "before dying". The specific epithet is an adjective that emphasizes the urgency of taxonomic efforts in conservation, highlighting the importance of describing species before they disappear or become extinct.

447

Distribution and natural history. Pristimantis praemortuus is known from the type locality in 448 the Chinambí sector and on the western slope of Cerro Golondrinas of the Dracula Reserve (Block 449 20) in the province of Carchi, between 2176 to 2390 meters of elevation, in the river basin. This 450 species is found in the montane evergreen forest of the Western Cordillera of the Andes (MAE 451 452 2013), characterized by a closed canopy with trees up to 20 meters high, covered by epiphytes, orchids, bromeliads, bryophytes, and ferns. The nine known specimens of Pristimantis 453 praemortuus were found active at night perching or vocalizing on fern leaves and bushes in the 454 lower and middle stratum of the forest, between 20 and 210 cm high. They were found in sympatry 455

with: P. pteridophilus complex, P. apiculatus, P. hectus, P. grp. devillei and P. satheri sp.nov.

456

- 457
- 458 Pristimantis broaddus sp. nov.
- 459 LSIDurn:lsid:zoobank.org:act:F060D100-C4EA-4882-BCFE-5EEBD8D9FFB0
- 460 Common name in Spanish: Cutin de Callie Broaddus
- 461 Suggested common English name: Broaddus'rainfrog

462

Holotype (Figs. 2, 5–8, 10–11). DHMECN 19037, adult female, from the Bosque Protector
 Golondrinas, El Pailón, El Goltal, Espejo, Carchi province, Ecuador, (0.81833, -78.09140; 2605
 m), collected on 27 July 2023 by at Miguel Urgilés-Merchán & Christian Paucar Veintimilla.

466

- **Paratypes** (Supp. Fig.1). A total of seven males (7) with the same type locality and the same data collection. DHMECN 19028, (0.82537, -78.09639; 2498 m); DHMECN 19029, (0.82534, -
- 469 78.09631; 2511 m); DHMECN 19031, (0.82365, -78.09532; 2483 m); DHMECN 19032,
- 470 (0.82483, -78.0962; 2499 m); DHMECN 19033, (0.82503, -78.0962; 2487 m); DHMECN
- 471 19034, (0.82361, -78.0949; 2512 m); DHMECN 19035, (0.82364, -78.0946; 2494 m) and one
- 472 juvenile (1): DHMECN 19036, (0.81995, -78.09433; 2570 m).

- **Diagnosis.** Pristimantis broaddus sp. nov. is a member of the Pristimantis myersi species group
- and *P. celator* species clade, characterized by the following combination of characters: (1)
- dorsal skin shagreen with scattered low tubercles and low warts, some aggregation of tubercles
- 477 extending towards the post sacral region; flanks with subconical tubercles aggregated mainly in
- 478 the axillary region; subconical tubercles on the ventral edge of the lower jaw; dorsolateral fold



479 present well-defined visible from the scapular region to or slightly beyond the sacral region (ilium), discoidal fold present slightly visible, belly areolate with tiny scattered tubercles; (2) 480 tympanum present, superficially visible, tympanic annulus weekly defined, round, horizontal 481 diameter of tympanum equal to 44,83% of eye diameter, antero-dorsal margin with a 482 483 supratympanic fold composed by low warts, subconical postrictal tubercles present; (3) snout short, broadly rounded in dorsal view, short, curved, curved, tip of snout protruding in lateral 484 view; (4) upper eyelid with one conical tubercle surrounded with several lower subconical 485 tubercles; cranial crest absent; (5) dentigerous processes of vomers positioned, obliques in 486 outline, posterior to level of choanae, minute and embedded in roof of mouth, barely visible and 487 therefore sometimes considered to be absent; (6) males unknown; (7) finger I shorter than finger 488 II; discs broad and expanded mainly in the fingers III-IV, with circummarginal grooves; (8) 489 fingers with strongly crenulated lateral fringes, mainly in Finger IV; (9) ulnar tubercles present. 490 subconical placed on the outer edge of the ulna; (10) heel with an elongated conical tubercle 491 492 surrounded by lower rounded tubercles, outer edge of the tarsus with a row of subconical 493 tubercles, internal tarsal fold weakly defined; (11) metatarsal tubercle slightly larger than the external one which is rounded and subconical; very few supernumerary tubercles and barely 494 visible; (12) toes with weakly defined lateral fringes, basally pronounced, interdigital membrane 495 absent, toe V longer than toe III, does not reach the base of the distal subarticular tubercle of the 496 IV toe; (13) Dorsal coloration back in light neutral gray to medium neutral gray (sayal brown to 497 burnt umber in life) with speckled marks disky brown or vandyke brow (spectrum green to dark 498 spectrum green in life). Ventrally pale neutral gray to dark neutral gray to light brown (with 499 warm sepia, scattered reddish-brown tubercles in life). Distinctive dark brown trapezoidal-500 501 shaped mark on the throat, bordered in cream, with a green outer heel edge and gold iris.

502 503

504 505

506

507

508 509

510

511

512

513

514

515

516

517 518 Comparison with other species (Fig. 2, 6–8). The new species differs from the most closely related species (P. verecundus, P. mutabilis, P. dracula sp. nov., P. satheri sp. nov., and P. praemortuus sp. nov.) by the presence of dorsolateral fold well-defined visible from the scapular region to or slightly beyond the sacral region (ilium) (complete dorsolateral glandular folds extending to the first quarter of the ilium in *P. satheri* sp.nov., dorsolateral fold reaching just before the sacrum in P. verecundus, dorsolateral fold only reach the level of sacrum in P. mutabilis, dorsolateral folds extending the entire length of the ilium in P. robayoi sp.nov.); a white belly without V-shaped markings on the throat (present in P. verecundus, P. broaddus sp.nov., P. praemortuus sp. nov., reduced or inconspicuous in P. mutabilis and P. robayoi sp.nov.; the dorsal surface of the tibia covered by transverse rows of glandular tissue in P. broaddus sp. nov., P. verecundus and P. praemortuus sp.nov. (outlining the extreme edge of the heel in *P. robayoi* sp.nov., and dorsal surface of tibia covered by glandular tissue in *P. satheri*); and a gold red in P. broaddus sp.nov. (bright orange-copper with a black edge in P. robayoi sp.nov., coppery gold in *P. praemortuus* sp.nov., iris cream to golden with thin black reticulation and a reddish-brown horizontal streak in *P. mutabilis*, and wine-colored in *P. satheri* sp. nov.). Tympanic annulus tympanic annulus weekly defined in *P. broaddus* sp.nov. (clearly defined,



round, posterior border of tympanic annulus with a thick fold in *P. praemortuus* sp.nov.), fingers with weakly defined lateral fringes in *P. broaddus* sp.nov.(fingers with lateral fringes, strongly crenulated mainly in finger IV in *P. praemortuus* sp.nov.), toes with weakly defined lateral fringes, basally pronounced, interdigital membrane absent in *P. broaddus* sp.nov. (toes with weakly defined lateral fringes, basally pronounced, interdigital membrane absent, outer edge of the foot and toe IV crenulated in *P. praemortuus* sp.nov.).

Genetic distances with close-related species (*Pristimantis broaddus* sp. nov. vs. *P. praemortuus* sp.nov.) have 3.54%. The genetic distances with other species in this clade range from 3.54%–12.49% (Supplementary Table 2)

Description of the holotype (Figs. 2, 5–8, 10). Adult female (DHMECN 19037), head longer than wide. snout short, broadly rounded in dorsal view, short, curved, curved, tip of snout protruding in lateral view, eye-nostril distance 9.82% of SVL, *canthus rostralis* slightly concave, defined, loreal region concave, nostrils protuberant, directed dorsolaterally; interorbital area slightly elevated, interorbital fold absent, interorbital distance wider than upper eyelid, 72.38%; cranial crest absent, X-shaped occipital crease (evident in life); upper eyelid with one conical tubercle surrounded with several lower subconical tubercles (reduced by preservation effects), tympanum present, superficially visible, tympanic annulus weekly defined, round, slightly visible dorsally, diameter of tympanum equals 49.23% of eye diameter, antero-dorsal margin with a supratympanic fold composed by low warts, subconical postrictal tubercles present; choanae small, rounded, not concealed by palatal shelf of maxilla; dentigerous processes of vomers positioned, obliques in outline, posterior to level of choanae, minute and embedded in roof of mouth, barely visible, two minute teeth. Tongue longer than wide, notched posteriorly, posterior 60% not adhered to mouth floor.

Texture of dorsum dorsal skin shagreen with scattered low tubercles and low warts, some aggregation of tubercles extending towards the post sacral region; flanks with subconical tubercles aggregated mainly in the axillary region; subconical tubercles on the ventral edge of the lower jaw; dorsolateral fold present well-defined visible from the scapular region to or slightly beyond the sacral region (ilium), discoidal fold present slightly visible, venter areolate with tiny scattered tubercles; two evident ulnar tubercles present, subconical placed on the outer edge of the ulna; outer palmar tubercle lobular, segmented into three parts, approximately the same size of elongated outer thenar tubercle; supernumerary tubercles present; subarticular tubercles defined, rounded in lateral view. Fingers strongly crenulated, mainly in Finger IV; Finger I shorter than finger II; discs broad and expanded mainly in the fingers III-IV, with circummarginal grooves, about 1.8× the size of the digit. Hind limbs slender (TL 47.02% of SVL; FL 44.6% of SVL); heel with an elongated conical tubercle surrounded by lower rounded tubercles, outer edge of the tarsus with a row of subconical tubercles, internal tarsal fold weakly defined; metatarsal tubercle slightly larger than the external one which is rounded and subconical; few barely visible supernumerary tubercles; toes with weakly defined lateral fringes, basally pronounced,



interdigital membrane absent, toe V, which is longer than toe III, does not extend to the base of the distal subarticular tubercle of toe IV.

Holotype coloration in preservative (Fig. 10). Background color in pale neutral gray (296) and light neutral gray (297). With distinctive medium dorsal mark dark grayish brown (284). Surface of the head and occipital region with spots in shades of Pinkish withe (216). Dorsolateral folds pale Pinkish buff (3). Delineated markings in sepia (286) and pale neutral gray (296) on the scapular region and dorsum. Ovoid markings on the flanks, diagonal bars on the posterior surfaces of the thighs, forearms, tibiae, and feet with markings in shades of drab (19) to dusky brown (285). Interspaces of bars on posterior surfaces of thighs and forearms pale neutral gray (296). Diagonal bars drab gray (256) extend from back of head to middle of flanks; anterior half of white with diagonal bars dusky brown (285). Inguinal region in spectrum orange background (9) and ventral surfaces of tibia in light fresh color (250). Ventrally pale neutral gray (296), finely punctuated with dark neutral gray (299); chest and inverted trapezoidal mark on throat dark neutral gray (299).

Holotype coloration in life (Fig. 6, 11). Anterior surface of the dorsum russet color (44) with distinctive occipital, loreal, posterior surfaces of the thighs, heels, and base of the fingers IV-III, apple green (104). Posterior surface of dorsum beige (254) with dorsolateral buff folds (5), flank bars pale lime green (112), ovoid flank markings, smoke gray (267). Bars on posterior surfaces of thighs and tibia, anterior flank markings, and supratympanic stripe ground cinnamon (270). Labial stripes cinnamon drab (50). Ventrally, dark pearl gray (280) with protruding ground cinnamon colored tubercles (270). Groin and anterior surfaces of the tibia poppy red (63). Trapezoidal marl on chin and lines on throat and ventral surface of thighs Dusky brown (285). Iris sulphur yellow (80).

Measurements (in mm) of holotype. SVL = 18.21; HW = 6.04; HL = 6.26; ED = 1.97; IOD = 2.11; EN = 1.79; TD = 0.97; TL = 8.15; EW = 1.52; FoL = 8.88; HaL = 4.75; FW = 0.54; TW = 0.57.

Variation. Morphometric variation in the type series (only females) is shown in Table 2 and Supplementary Fig. 3. Variations in coloration in life (Fig. 11), dorsal coloration from sayal brown (41) (DHMECN 19029, 19035) to burnt umber (48) (DHMECN 19031, 19036), with distinctive diagonal stripes on the flanks ranging from straw yellow (53) (DHMECN 19029) to pale cinnamon (54) (DHMECN 19035), bordered in cream. The dorsum with speckled marks of spectrum green (129) (DHMECN 19028, 19029, 19037) to dark spectrum green (130) (DHMECN 19036), dorsolateral folds straw yellow (53) (DHMECN 19035, 19028), pale cinnamon (54) (DHMECN 19029), or true cinnamon (260) (DHMECN 19036). Black supratympanic stripe with cream anterior border, irregular and incomplete, does not reach the postrictal tubercle. Labial stripes burnt umber (48) (DHMECN 19029, 19035) or jet black (300)



(DHMECN 19036) and transversal tibial (glandular) straw yellow to pale cinnamon (54)
(DHMECN 19035, 19028, 19036). Outer heel edge spectrum green (DHMECN 19035, 19028,
19036). Trapezoidal mark on chin from Dusky brown (285) (DHMECN 19037), amber (51),
(DHMECN 19035) to sepia (286), separated by bars, dark pearl gray (280), pales horn color (11)
and olive horn color (16). Ventrally dark pearl gray (280) (DHMECN 19037), pale neutral gray
(296) (DHMECN 19035) to olive brown (278) (DHMECN 19036), speckled with warm sepia
(40), scattered reddish-brown tubercles.

In preservative (Supplementary material Fig. 4), anterior dorsal pattern varies from back in light neutral gray (297) (DHMECN 19037) to medium neutral gray (298), (DHMECN 19031–32, 19035). Medium dorsal mark from dark grayish brown (284) (DHMECN 19037) with dusky Brown (285) (DHMECN 19031–32, 19028) and vandyke brown (281) (DHMECN 19028). Specimen DHMECN 19036 with white middorsal stripe extending from snout to the vent. Flanks with dorsolateral oblique bands and, shades of drab (19) (DHMECN 19037), beige (254) (DHMECN 19035) to vandyke brown (281) (DHMECN 19031–32). Groin and anterior surfaces of the tibia vary from poppy red (63) (DHMECN 19037), spectrum orange (9) (DHMECN 19032) to salmon (251) (DHMECN 19031). Belly varies from pale neutral gray (296) (DHMECN 19032) with dark spots scattered to dark neutral gray (299) (DHMECN 19031), with heavy mottled reaching throat, chest, and ventral limbs. Specimen DHMECN 19036, ventral coloration extending on the waist delineating a trapezoidal mark shape jet black (300). Specimen DHMECN 19035 is the only specimen with V mark shape.

Etymology. The specific epithet *broaddus* is a noun in apposition in recognition of Callie Broaddus. She is an American conservationist, photographer, and filmmaker. Founder of Reserva: The Youth Land Trust, a nonprofit organization that empowers youth to conserve threatened species and habitats. Since 2019, she has worked primarily in the Tropical Andes of Ecuador, collaborating with local partners to protect the Dracula Reserve ecological corridor. Callie has a strong background in conservation and youth activism, with experiences from various international expeditions and conferences. Previously, she was a senior designer at National Geographic Kids and has been involved in multiple outreach and environmental education projects.

 Distribution and natural history. *Pristimantis broaddus* sp. nov. is known only from the type locality in the El Pailón sector, of the Golondrinas Protective Forest of the province of Carchi, between 2483 to 2605 meters of elevation, in the Mira River Basin located on the slope of Cerro Golondrinas. This species is found in the montane evergreen forest of the Western Cordillera of the Andes (MAE 2013), characterized by a semi-open canopy up to 20 meters high, covered by epiphytes, orchids, bromeliads, bryophytes, and ferns, with dominance of suros (*Chusquea sp*). The nine known specimens of *Pristimantis broaddus* sp. nov.were found in the lower layer of the forest between 10 and 110 cm, on leaves of bushes and ferns at night. *P. broaddus* are found in



- sympatry with the species; *Pristimantis celator*, *P. pteridophilus complex*, *P. apiculatus*, and *P. hectus*.
- 640 Pristimantis satheri sp. nov.
- 641 Eleutherodactylus verecundus Lynch & Burrowes, 1995. Occas. Pap. Mus. Nat. Hist. Univ.
- 642 Kansas, 136: In Part: Paratype: IAvH-Am-1492.
- 643 Pristimantis sp.5 Franco-Mena et al. 2023
- 644 LSIDurn:lsid:zoobank.org:act:D756EFAA-9D18-4564-AB7F-B5E1866054E0
- 645 **Proposed standard Spanish name:** Cutin de Justin Sather.
- 646 Proposed standard English name: Satheri's rainfrog

- Holotype (Fig. 2, 5–8, 12–13). DHMECN 14858, adult female, from San Jacinto de Chinambí,
 Jijón y Caamaño, Tulcán, Carchi province, Ecuador, (0.860927, -78.272364; 2156 m), collected
- on 15 June 2019, by at Mario H. Yánez-Muñoz; Mateo Vega-Yánez and Daniel Padilla.

651

- **Paratypes** (Supp. Fig. 4). A total of five specimens (5). Adult females (1): DHMECN 14885,
- with the same type locality and data collectors, (0.861354, -78.276026; 2196 m.), collected on 17
- June 2019; Adult males (2): DHMECN 16578, from Bloque 18, Dracula Reserve, Tulcán, Carchi
- 655 province, Ecuador, (0.87830 -78.20604; 2141 m), collected on 15 October 2021 by at Ross
- 656 Mayner & Jaime Culebras; DHMECN 19538, from the Bloque 20, Dracula Reserve, Tulcán,
- 657 Carchi province, Ecuador, (0.83566, -78.22842; 2394 m), collected on 5 December 2023 by at
- 658 Mario H. Yánez-Muñoz; Christian Paucar Carlos Ríos & Miguel Urgilés-Merchán; Juveniles (2):
- DHMECN 16574, with the same data of DHMECN16578; DHMECN 17903, Cerro Negro,
- Dracula Reserve, Carchi province, Ecuador, (0.8826, -78.19587; 1742 m), collected on 5 August
- 661 2022 by at Gabriela Lagla-Chimba, Julio César Carrión-Olmedo & Milton Cantincuz.

- **Diagnosis.** Pristimantis satheri sp. nov. is a member of the Pristimantis myersi species group
- and P. celator species clade, characterized by the following combination of characters: (1) dorsal
- skin shagreen with flanks with rounded warts, venter areolate, discoidal fold present and visible
- posteriorly, dorsolateral glandular folds complete, from the scapular region to the first quarter of
- the ilium; (2) tympanum present, superficially visible, tympanic ring well defined, round,
- 668 horizontal diameter of tympanum equal to 34,11% of eye diameter and without conical tubercles;
- 669 (3) snout short, subacuminate in dorsal view, rounded in profile with slightly flared [2] lips; (4)
- of upper eyelid with several small rounded tubercles; no cranial crest; (5) dentigerous processes of
- the vomer present, triangular in outline each process with 4 5 teeth; (6) vocal slits present; with
- 672 nuptial pad and low vocal sac; (7) finger I shorter than finger II; broad, expanded, disks dilated
- with circummarginal grooves; (8) fingers with thin lateral fringes, strongly crenulated on external
- edge of finger IV extends and attenuates to finger III; (9) ulnar tubercles present, with 3–4
- 675 rounded tubercules; (10) heel with one subconical tubercle; outer edge with two subconical
- tubercles, dorsal surface of the tibia covered by glandular tissue; (11) small inner metatarsal



tubercle oval 2 times larger than small rounded outer metatarsal tubercle; supernumerary tubercles lows; (12) toes with thin cutaneous lateral fringes, interdigital membrane absent, toe V longer than toe III, fringes developed and thick on the fingers, edge of toe V crenulated; (13) dorsally, from light green with a variegated pattern of black, with distinctive orange dorsolateral folds and tibial gland, to grayish brown; white belly without distinctive V-shaped markings; (14) small adult males, SVL= 19.73-19.79 mm (mean = 19.76, *n*= 2), females SVL= 22.08-23.74 mm (mean = 22.91 mm, *n*= 2), Juveniles, SVL= 14.7-14.71 mm (mean = 14.71 mm, *n*= 2).

Comparison with other species (Figs. 2, 5–8). The new species differs from other species of the clade (*P. verecundus*, *P. mutabilis*, *P. robayoi* sp. nov., *P. broaddus* sp. nov., and *P. praemortuus* sp. nov.) by the presence of complete dorsolateral glandular folds extending to the first quarter of the ilium (partial dorsolateral folds reaching just before the sacrum in *P. verecundus*, dorsolateral folds reaching the sacrum in *P. broaddus* sp. nov. and *P. praemortuus* sp.nov., only reach the level of sacrum in *P. mutabilis*, dorsolateral folds extending the entire length of the ilium in *P. robayoi* sp. nov.; a white belly without V-shaped markings on the throat (present in *P. verecundus*, *P. broaddus* sp.nov., *P. praemortuus* sp.nov., reduced or inconspicuous in *P. mutabilis* and *P. robayoi* sp. nov.); and the dorsal surface of the tibia covered by glandular tissue (outlining the extreme edge of the heel in *P. robayoi* sp.nov., and in transverse rows on the tibia in *P. verecundus*, *P. broaddus* sp.nov., and *P. praemortuus* sp.nov.); and a red wine-colored iris (bright orange-copper with a black edge in *P. robayoi* sp. nov., coppery gold in *P. praemortuus* sp. nov., gold in *P. broaddus* sp. nov., iris cream to golden with thin black reticulation and a reddish-brown horizontal streak in *P. mutabilis*).

 Genetic distances with close-related species (*Pristimantis satheri* sp. nov. vs. *P.* csp.2) have 11.14%. The genetic distances with other species in this clade range from 10%–14% (Supplementary Table 2)

Description of the holotype (Fig. 12–13). Adult female 23.7 mm SVL. Head longer than wide, snout short, subacuminate in dorsal and lateral view, eye-nostril distance 84.39% of horizontal eye diameter. Canthus rostralis straight, defined, loreal region concave, narines directed slightly posterior laterally; interorbital area flat, no interorbital fold, interorbital distance wider than upper eyelid, 76.33%; no cranial crest. Upper eyelid bearing small rounded tubercles, tympanum present, tympanic membrane not differentiated from surrounding skin, tympanic ring slightly evident bellow skin, upper margin covered by low tympanic fold, tympanum visible dorsally, diameter of tympanum equals 33.75% of eye diameter, underside of tympanum with three enlarged rounded tubercles; choanae small, oval in outline, not covered by palatal floor of maxilla; dentigerous processes of vomers present, triangular oblique in outline with 4 to 5 teeth, tongue longer than broad as broad as long, oval in shape 40% attached to floor of mouth.

Texture of dorsum finely granular with a pair of small rounded tubercles in occipital area, complete dorsolateral glandular folds with some rounded tubercles along the folds, flanks strongly rough with small rounded warts widespread on the flanks; belly strongly areolate;



- discoidal fold weakly evident, cloaca with finely granular texture. Slender arms with thick glandular skin, lor rounded tubercles on dorsal and ventral surface of forearm. Ulnar tubercles present; small subconic and rounded; broad truncated disks on fingers II to IV, finger round slightly expanded, all fingers bearing circummarginal grooves, subarticular tubercles rounded and flattened in lateral view, fingers with thin lateral cutaneous ridges; tenar tubercle oval enlarged with some irregular borders almost half size of palmar "horseshoe" shape tubercle, palmar surface with low flat and inconspicuous supernumerary tubercles; hind limbs slender, length of tibia equals 49.03% of SVL, glandular patch on outer surface of tibia; enlarged rounded tubercles on the heel surrounded by small tubercles, row of rounded tubercles along outer edge of the tarsus, inner tarsal fold absent, toes with thin cutaneous ridges, toes I to V widely expanded bearing circummarginal grooves without digital membranes; subarticular tubercles rounded and flattened in profile view; expanded disks on all toes, larger than those of the hand. Toe V longer than III, not extending beyond subarticular tubercle of toe IV.
 - Holotype coloration in preservative (Fig. 12). Dorsal surface, forelimbs, and hindlimbs ferruginous (color 35) background, with a thin sepia (color 279) interorbital, dorsal, forelimbs, and hind limb with bands. Dorsolateral glandular folds and glandular folds light yellow ocher (color 13). Flanks and dorsal surface of hindlimbs olive brown bands (color 278), finely outlined in white with interspaces clay color (color 20). Smoky white (261) belly, finely dotted with smoke gray (267). Ventral surface of thighs and legs, variegated with smoke gray (267). Sepia (279) canthal, supralabial and supratympanic markings.
- Holotype coloration in life (Fig. 13). Dorsal coloration on a light buff background (2), with
 distinctive marks and light pistachio outlines (101). Dorsolateral glandular folds and glandular
 folds flame scarlet (73). Belly and throat pale neutral gray (297), with cream spots. Dorsal
 markings, supratympanic lines, labial bars, flank bars, front and hind limbs jet black (color 300).
 Gem Ruby (65) colored iris.
- **Measurements (in mm) of holotype.** SVL = 23.74; HW = 8.51; HL = 9.23; ED = 3.14; IOD = 746 2.62; EN = 2.65; TD = 1.06; TL = 11.63; EW = 2; FL = 11.86; HaL = 7.13; FW = 1.27; TW = 1.04.
 - **Variation.** *Pristimantis satheri* sp. nov shows sexual dimorphism in body size (Fig. supp. 3), females 0.86 times larger than males (Supplementary, Fig. 3). Other morphometric variations of the type series are showing in Table 2.
 - In life (Fig. 13), dorsal background coloration ranges from light buff (2) with pistachio markings (101) (DHMECN 14858) to cinnamon drab (21) with drab-gray markings (256) (DHMECN 14885). The dorsal glands are observed to exhibit a range of colors, including flame scarlet (73) (DHMECN 14858), medium chrome orange (75) (DHMECN 17903), and drab-gray (256) (DHMECN 14885). Dorsal end bars are jet black (300) or in lighter shades (DHMECN



14858), or they may be true cinnamon (260) (DHMECN 17903). The ventral surface is characterized by a neutral gray background (297) (DHMECN 14858, 14885) with cream-colored 758 spots or a uniform cream color (12) (DHMECN 17903). 759

In preservative (Supplementary Fig. 5), dorsally the background color varies from ferruginous (35) (DHMECN 14858), mahogany red (34) (DHMECN 16578) to true cinnamon (260) (IAvH-Am-1492). Bars on the posterior surfaces of the thighs sepia (279) (DHMECN 16578), russet (44) (DHMECN 19538), true cinnamon (260) (IAvH-Am-1492).

763 764 765

766

767

768 769

757

760 761

762

Etymology. The specific name *satheri* is a noun in the genitive case and is a patronym Justin Sather. Justin, a 13-year-old American male, is an ardent environmentalist. Justin Sather was inspired to found the Justin's Frog Project by a dual concern: his love for frogs and the decline of their populations due to pollution and habitat destruction. He has safeguarded over 100 acres of rainforest in Ecuador, removed 1,000 pounds of waste from polluted rivers, and planted 500 trees. Justin's objective is to foster awareness and prompt action to safeguard the planet.

770 771

Distribution and natural history. Pristimantis satheri is known in the type locality in the San 772 Jacinto de Chinambi sector, block 18 and block 20 of the Dracula Reserve, in the province of 773 Carchi, between 1742 and 2394 meters elevation, in the Mira River Basin. This species is found 774 775 in the evergreen montane forest of the Western Cordillera of the Andes (MAE 2013). characterized by an open canopy with trees up to 20 meters high, covered by epiphytes, orchids, 776 bromeliads, bryophytes, and ferns. The six known specimens of Pristimantis satheri were found 777 778 active at night perching on leaves of shrubs and bromeliads in the lower and middle stratum of 779 the forest, between 100 to 180 cm in height. They were found in sympatry with: P. pteridophilus complex, P. apiculatus, P. hectus, P. grp. devillei and P. praemortuus sp. nov.. (Fig. 3). 780

781

- 782 Pristimantis robayoi sp. nov.
- 783 Eleutherodactylus verecundus Lynch & Burrowes, 1995. Occas. Pap. Mus. Nat. Hist. Univ.
- Kansas, 136: In Part: Partype: IAvH-Am-1801. 784
- LSIDurn:lsid:zoobank.org:act:FC56EB54-455A-4FCD-B2AD-0CAE25B12B47 785
- Common name in Spanish: Cutín de Robayo 786
- 787 Suggested common English name: Robayo's rainfrog.

788

789 Holotype (Figs. 2, 6–8, 14–15). DHMECN 17894, adult female, from the Dracula Reserve, Chical, Tulcán, Carchi province, Ecuador, (0.86771, -78.19961; 2070 m), collected on 2 August 790 2022 by Gabriela Lagla-Chimba, Julio Cesar Carrión & Milton Cantincuz. 791

- 793 **Paratypes** (Fig. supp. 3). A total of fourteen specimens of the type series. Adult females (7):
- Adult females DHMECN 14884, from San Jacinto de Chinambí, Jijón y Caamaño, Tulcán. 794
- 795 Carchi province, Ecuador, (0.860927, -78.272364; 2156 m), collected on 15 June 2019, by at
- 796 Mario H. Yánez-Muñoz; Mateo Vega-Yánez and Daniel Padilla.; DHMECN 14947, DHMECN



818 819

820

821

822 823

824

825

826 827

828

829

830

831

832

833

834 835

836

797 14948 and DHMECN 14960 from sendero al río Cumbe, Maldonado, Tulcán, Carchi province, Ecuador, (0.89704, -78.11841; 2012 m), collected on 24 October 2019 by at Miguel Andrés 798 Urgilés Merchán, Mateo Vega Yánez, Cristian Daniel Agila & Rafael Mena: DHMECN 16573. 799 from the Cerro Negro, Dracula Reserve, Chical, Tulcán, Carchi province, Ecuador, (0.87663, -800 801 78.20535; 2160 m), collected on 15 August 2021 by Ross Maynard; DHMECN 19429, from the Dracula Reserve, Cerro Golondrinas, Chical, Tulcán, Carchi province, Ecuador, (0,86623, -802 78,20392; 2227m), collected on 16 September 2023 by Juan Pablo Reyes-Piug. Adult males (3): 803 DHMECN 14979, with the same data of DHMECN 14960; DHMENC 16150, from the La 804 Esperanza, Quinshul, Tulcán, Carchi province, Ecuador, (0.92704, -78.24178; 1979 m); collected 805 806 on 27 March 2021 by Mario H. Yánez-Muñoz & Juan P. Reves; DHMECN 16567 with same data of 14960. Juvenil (4): DHMECN 14886, from the Rio Chinanbi, San Jacinto de Chinanbi, 807 Mira, Carchi province, Ecuador, (0.861354, -78.275964; 2193 m), collected on 17 June 2019 by 808 at Mario Humberto Yanez Muñoz, Mateo Vega Yánez & Daniel Padilla; DHMECN 14950, from 809 810 the Dracula Reserve, Cerro Golondrinas, Chical, Tulcán, Carchi province, Ecuador (0.89704, -78.11841; 2012 m), collected on 16 September 2023 by Juan Pablo Reyes-Piug; DHMECN 811 14953, (0.89704, -78.11841; 1791 m), from Sendero al río Cumbe, Maldonado, Tulcán, Carchi 812 province, Ecuador, collected on 24 October 2019 by at Miguel Andrés Urgilés Merchán, Mateo 813 814 Vega Yánez, Cristian Daniel Agila & Rafael Mena; DHMECN 16575, from the Dracula Reserve, Chical, Tulcán, Carchi province, Ecuador, (0.87635, -78.20551; 2161 m), collected on 815 15 August 2021 by Ross Maynard. 816

Diagnosis. Pristimantis robayoi sp. nov. is a member of the Pristimantis myersi species group and P. celator species clade, characterized by the following combination of characters: (1) complete dorsolateral folds, extending below occipital region through the scapula to the ilium, with a pair of occipital and scapular short sub-conical tubercles, flanks with small, low warts aligned dorsolaterally, flattened warts, areolate belly, discoidal fold present and visible posteriorly, dorsolateral folds finely defined; (2) tympanum hidden below the skin, tympanic annulus present, round, well-defined, horizontal diameter of the tympanum equal to 33.13% of the eye diameter, postrictal sub-conical tubercles present; (3) snout short, rounded in dorsal and profile views; (4) upper eyelid with several low sub-conical tubercles and one small conical tubercle, small rounded interobital tubercle; no cranial crest; (5) vomerine odontophores present, triangular in outline, each odontophore with 7-9 teeth; (6) vocal slits not visible; nuptial pad absent, no vocal sac; (7) Finger I shorter than Finger II; expanded discs wider than the digits, fingers with circumferential grooves and lateral fringes; (8) sub-conical ulnar tubercles present; (9) heel with a sub-conical tubercle surrounded by lower ones, three tubercles on the edge of the tarsus, glands present outlining the outer edge of the heel; (10) two metatarsal tubercles, inner metatarsal tubercle oval, three times the size of the outer sub-conical one, low supernumerary tubercles present: (11) toes with lateral fringes that widen basally, no interdigital membrane: (12) dorsally dark brown with distinctive black scapular marks, dorsolateral folds, diagonal bands on the flanks, postrictal area, and glandular surface of the outer edge of the heel orange-brown,



diagonal labial bars, black supratympanic fold, belly light brown to dark brown densely speckled, iris bright orange-copper with a black edge.

838 839 840

841

842

843

844

845

846

847

848

849

850

851

852

853 854

855

856

857

858 859

860

861

862 863

837

Comparison with other species (Fig. 2, 6–8). The new species differs from its closest nominal lineages (P. verecundus, P. mutabilis, P. satheri sp. nov., P. broaddus sp. nov., P. praemortuus sp. nov.), by complete dorsolateral folds, extending below occipital región through the scapula to the illium (complete dorsolateral glandular folds extending to the first quarter of the ilium in P. satheri, dorsolateral fold reaching just before the sacrum in P. verecundus, dorsolateral fold only reach the level of sacrum in P. mutabilis, dorsal fold present well-defined visible from the scapular region to or slightly beyond the sacral region (ilium) in P. boraddus sp. nov.); a with belly areolate (belly without V-shaped markings on the throat in P. praemortuus sp. nov., P. verecundus, P. broaddus sp. nov., reduced or inconspicuos in P. mutabilis and P. satheri sp. nov.); glands present outlining the outer edge of the heel (dorsal surface of tibia covered by glandular tissue in P. satheri sp. nov., dorsal surface of the tibia covered by transverse rows of glandular tissue in P. broaddus sp. nov., P. verecundus and P. praemortuus sp. nov.); iris bright orange-copper with a black edge (gold red in P. broaddus sp. nov., coppery gold in P. praemortuus sp. nov., iris cream to golden with thin black reticulation and a reddish-brow horizontal streak in *P. mutabilis*, and wine-colored in *P. satheri* sp. nov.); Tympanum hidden below the skin, tympanic annulus present, round, well-defined (tympanum present, superficially visible, tympanic ring well defined, round in P. satheri sp. nov., tympanic annulus clearly defined, round, posterior border of tympanic annulus with a thick fold in *P. praemortuus* sp. nov., tympanic annulus weakly defined in *P.broaddus* sp. nov.). Fingers with skin ridges that widen mainly at the base of fingers I-II and II-III, absent interdigital membrane (toes with thin cutaneous lateral fringes, interdigital membrane absent, toe V longer than toe III, fringes developed and thick on the fingers, edge of toe V crenulated in P. satheri sp. nov., fingers with lateral fringes, strongly crenulated mainly in finger IV in P. praemortuus sp. nov., fingers with weakly defined lateral fringes in *P. broaddus* sp. nov.).

864 865 Genetic distances with close-related species (*Pristimantis robayoi* sp.nov. vs. *P. verecundus*) have 8.81%. The genetic distances with other species in this clade range from 8.08%–14.79% (Supplementary Table 2)

866 867 868

869

870

871

872

873

874

875 876 **Description of the holotype** (Figs. 14). Adult male (DHMECN 17894), head longer than wide. Snout short, rounded slightly elongate, short and rounded in profile; eye-nostril distance 10.08% of SVL, *canthus rostralis* is weackly concave in dorsal view, whereas in cross section is rounded, loreal region concave, slightly protuberant narines directed laterally; interorbital area flat, no interorbital fold, interorbital distance wider than upper eyelid, 63.1%; no cranial crest; upper eyelid with small subconic tubercles, cona small rounded interorbital tubercle; tympanum and tympanic annulus evident, tympanic membrane differentiated from surrounding skin, tympanic, not visible in dorsal view; low supra tympanic fold extending from postocular to the level of the insertion of the arm; diameter of tympanum equals 33.13% of eye diameter,





underside of tympanum with low rounded postrictal tubercles; choanae small, rounded in outline, not covered by palatal floor of maxilla; dentigerous processes of vomers present oblique in outline no teeth evident, tongue as broad as long, oval in shape 40% attached to floor of mouth.

Texture of dorsum is finely granular with low "W" shape fold on the occipital region, the fold is not evident on preserved specimen, a pair of small subconic tubercles in occipital and scapular areas, low dermal ridges extending posterior to the supratympanic and occipital folds. connecting to the complete dorsolateral fold, pairs of low rounded warts are present along dorsolateral folds; flanks finally granular with low rounded tubercles, belly areolate with rounded tubercles, throat granular with low rounded tubercles; discoidal fold not evident; cloaca with granular texture; slender arms with low rounded tubercles es on dorsal surface of forearm. Low rounded ulnar tubercles; broad truncated disks on fingers II to IV, rounded and slightly expanded on finger I, al disks with circummarginal grooves, subarticular tubercles rounded and flattened in lateral view, all finger with thin lateral fringes; tenar tubercle oval and widely elongated, "V" irregular shape palmar tubercle, palmar surface with scarce low rounded small supernumerary tubercles, hind limbs slender, length of tibia equals 53.09% of SVL, no tubercle on outer edge of tibia, small subconical tubercle present on the heel, low inner tarsal fold present; toes with thin lateral fringes without digital membranes; subarticular tubercles rounded and flattened in profile view; expanded truncated disks on all toes except on toe I is oval. Toe V longer than III, not reaching distal subarticular tubercle of toe IV.

Holotype coloration in preserved (Fig. 14). Dorsal surfaces are heavily pigmented with dark neutral gray (299) small punctuations, limbs bears dull banded pattern alternated light neutral gray (297) with brownish olive (292), light neutral gray; pale neutral gray (296) light irregular interorbital mark, dark dusty brown (285) suborbital and supratympanic stripes present, small black marks surrounding occipital and scapular tubercles, light cream lines extending along dorsolateral folds; flanks with oblique banded pattern altering dark and gray tones, cloacal ornamentation composed by a dark gray trapezium mark delineated by white lines; fingers, toes and digital pads dull black. Ventral coloration of abdomen ends belly dark neutral gray (299), same as ventral limbs, palm, and soles; throat and chest white light pale coloration with dark spots on the chin; ventral shanks white pale coloration.

Holotype coloration in life (Fig. 15). Dorsal surfaces including forelimbs and hindlimbs predominant crimson (color 62), with antique brown (color 24), pale medium orange chrome 75 diffuse marks on interorbital area, dusky brown 285 on subocular and supratympanic stripes; pale medium orange chrome 75 along dorsolateral folds, heels and interspaces of banded pattern in the flanks that is mixed with chestnut 30, black marks surrounding occipital and scapular areas, iris golden with small black points and reticulations; ventral surfaces of body and limbs dark brown burnt amber (color 48), throat mottled with amber (Color 51).



Measurements (in mm) of holotype. SVL = 24.22; HW = 8.57; HL = 9.51; ED = 3.38; IOD = 918 2.9; EN = 2.44; TD = 1.12; TL = 12.86; EW = 1.83; FoL = 11.7; HaL = 7.58; FW = 1.3; TW= 919 1.24.

Variation. *Pristimantis robayoi* sp. nov. shows sexual dimorphism in body size (Supplementary Fig. 3), with females 0.8 times larger than males. Other morphometric variations of the type series are shown in Table 2.

In life (Fig. 15), the dorsal pattern of coloration on a brown background exhibits a range of variations, including warm sepia (40) (DHMECN 17894), kingfisher red-brown (28) (DHMECN 14947, 14960), and orange-brown tones such as salmon (58). (DHMECN 14884), Flesch ocher (57) (DHMECN 14948), chamois (84) (DHMECN 16150), and flame scarlet (73) (DHMECN 14885). The posterior flank spaces are enclosed by transverse bands that exhibit the same variation as the dorsum. Specimen DHMECN 14950 exhibits smoky white markings (262) between the posterior part of the eyelids and the skull. Additionally, specimen DHMECN 14948 displays cream color shades (12) in the mid-dorsal area, extending from the nape to the cloacal region. The ventral background coloration exhibits variation, from light yellow ocher (13) on the chest, throat, and chin, to cinnamon (21) without dots (DHMECN 14885), to cinnamon drab (21) (DHMECN14960), flesh ocher (57) (DHMECN14884) with dark melanophores and sepia-colored dots that are uniformly distributed on the ventral surface, including the throat and limbs.

In preserved specimens (Supplementary Fig. 6), the dorsal surface exhibits a variation in coloration, with dark melanophores that are jet black (300) (DHMECN 19429) or dark neutral gray (299) (DHMECN 16575). Additionally, the coloration of the surface of the dorsum exhibits a medium neutral gray (298) (DHMECN 14960), progressing to dark brown tones such as olive brown (278) (IAcH1801) or true cinnamon (260) (DHMECN 14979).

Etymology. The specific name *robayoi* is a noun in the genitive case and is a patronym for F. Javier Robayo. Javier Robayo is the President of Fundación EcoMinga in Ecuador, a nonprofit dedicated to conserving the country's rich biodiversity. He has played a pivotal role in protecting over 27,000 acres of critical habitats in the Chocó and Tropical Andes. As a biologist and educator, Robayo has led more than 200 research and teaching expeditions, contributing significantly to scientific discoveries, including new species of orchids, frogs, and rodents. His dedication extends to educating young researchers and fostering the next generation of conservationists.

 Distribution and natural history. *Pristimantis robayoi* it is known from three type localities: San Jacinto de Chinambi, Chical, and Maldonado in the province of Carchi, between 1791 and 2193 m elevation, in the Mira River basin. This species is found in the evergreen montane forest of the Western Cordillera of the Andes (MAE 2013), characterized by an open canopy with trees up to 20 meters high, covered by epiphytes, orchids, bromeliads, bryophytes, and ferns. The 14 known specimens of *Pristimantis robayoi*, were found active at night perching on leaves of



shrubs, bromeliads, and ferns in the lower stratum of the forest, between 60 to 160 cm high. They were found in sympatry with: *P. apiculatus*, *P. hectus*, *P. actites*, *P. quinquagesimus*.

Discussion

The polymorphic cryptic Type Series of *Eleutherodactylus verecundus* Lynch & Burrowes, 1990. The original description of this species (onwards *Pristimantis verecundus*) was based on seven specimens (the holotype and six paratypes), it provides an expanded general diagnosis of the interspecific variation of the species without details of life variations patterns. During the revision of Colombian *Pristimantis* material on ICN, one of the original authors of *P. verecundus* (John D. Lynch, personal communication) had previously noted concerns regarding the lack of individual information and completeness of the data collected at the type locality, Reserva La Planada. This limitation affected the understanding of inter- and intraspecific variation within the type series, complicating subsequent revisions in the compendium of western Ecuador (Lynch & Duellman, 1997), which considers *P. verecundus* as a widely distributed species from northwestern central Ecuador to extreme southwestern Colombia, but later contradicted with the description of *Pristimantis mutabilis* Guayasamín *et al.* 2015, actual phylogenies (Franco-Mena *et al.* 2023) and present work.

Our study, which involved delimiting species from Ecuador and examining the type material deposited at the IAvH in Colombia, confirms that the type series includes two of our four new species described in this work. Specifically, paratype IAvH-AM-1492 corresponds to the taxonomic identity of *Pristimantis satheri* sp. nov. characterized by the presence of rough glandular patches on dorsal surfaces, more rounded and smooth snout; while IAvH-AM-1493 belongs to *P. robayoi* sp. nov., diagnosed by complete dorsolateral fold extending to the ilium, rather than the holotype of *P. verecundus* with more acuminated and tuberculated snout and incomplete dorsolateral folds reaching below the sacrum.

The original description, not being strictly based on the holotype. For a better understanding of species limits and intraspecific variation, the redescription of *Pristimantis verecundus* is provided as supplemental material 2 and as Appendix 2, a species identification key to its phylogenetically related species.

Phylogenetic hypotheses related to the *Pristimantis celator* **species group.** Lynch and Duellman (1997) originally assigned *Pristimantis celator* and *P. verecundus* to the *P. unistrigatus* species group, based on the Toe Condition type C (fifth toe much longer than third). This is in contrast with Toe Condition type B (fifth toe longer than third but not extending to distal subarticular tubercule of fourth toe) in the *Pristimantis myersi* group.

Subsequently, Hedges *et al.* (2008) and Padial *et al.* (2013) employed *sensu stricto* sequences of *Pristimantis celator* and *sensu lato* sequences of *P. verecundus* (see phylogenetic comments on the *Pristimantis celator* clade) to ascertain the proximity between these species and the group of *Pristimantis myersi* species. Nevertheless, Hedges *et al.* (2008) maintained their



classification as species of the *unistrigatus* species group. Subsequently, Padial *et al.* (2013) excluded them from the proposed groups until the publication of their findings.

Guayasamin *et al.* (2019) conducted a study to determine the species limits between *Pristimantis mutabilis* and *P. verecundus sensu lato*. They assigned these species to the *Pristimantis myersi* species group and identified high support for their phylogenetic hypothesis. Subsequently, Franco-Mena *et al.* (2023) consolidated the *Pristimantis verecundus* clade based on extensive phylogenetic sampling and determined high cryptic diversity, associated with polytomy with *Pristimantis jubatus* and the species of the *Pristimantis myersi* group (see phylogenetic comments on the *Pristimantis celator* clade).

Our hypothesis consolidates the clade of *Pristimantis celator* species taxonomically and phylogenetically, like Franco-Mena *et al.* (2023), we found high cryptic diversity and consolidated *sensu stricto* sequences of *Pristimantis verecundus* in agreement with the morphological features of the holotype. In contrast, we reorganized the clade and placed it within the *Pristimantis myersi* species group (*P. myersi* subclade+*P. celator* clade+*P. jubatus* clade) and the *Trachyphrynus* subgenus (see phylogenetic comments on the *Pristimantis celator* clade). According to the protocol of Vences *et al.* (2013) and to other global trends of maintaining taxonomic stability of hyperdiverse groups of anurans (e.g. Mahony *et al.* 2024), we consider that our phylogenetic hypothesis is consistent with previous work (Hedges *et al.*, 2008; Rivera-Correa & Daza 2016; Gonzalez *et al.*, 2017; Jetz & Pyron 2018; Bejarano *et al.*, 2022) supporting the *Trachyphrynus* clade as a monophyletic group equivalent to a subgenus composed of four groups of species (*P. myersi* + *P. devillei* + *P. letolophus* + *P. boulengeri*).

We agree with recent phylogenetic studies in identifying morphological synapomorphies within the groups or subgenera of *Pristimantis*. Additionally, the four groups that constitute the subgenus *Trachyphrynus* may exhibit homoplastic characters across the *Pristimantis* genus. These include cranial crests (*devillei* group), iridophores (*boulengeri* group), hyperdistal tubercles (*leptolophus* group), and finger conditions B and C (two conditions in the *myersi* group), all found within various monophyletic groups of *Pristimantis* (Ospina-Sarria & Duellman, 2019; Ron *et al.*, 2024; Bejarano-Muñoz *et al.*, 2022).

Hypothesis of speciation and radiation of the *Pristimantis celator* clade. The role of mountain systems, such as the Andes, in driving species diversification is further corroborated by studies on the geological and evolutionary processes shaping mountain biodiversity (Antonelli *et al.*, 2018; Perrigo *et al.*, 2019; Hoorn *et al.*, 2019). As detailed by Hoorn *et al.* (2019), the orogeny of mountain ranges, including the Andes, has created complex landscapes that serve as hotspots for both allopatric and sympatric speciation.

The phylogenetic analysis of the *Pristimantis celator* clade (14 species) reveals a distinct radiation confined to the western slopes of Ecuador and the southernmost region of Colombia. Specifically, 64% of the clade (9 species) inhabit montane forests at elevations ranging from 1400 m to 2300 m in the binational basin of the Mira River. In contrast, 36% (6 species) occupy similar elevations, including the Andean foothills up to 600 m in the Esmeraldas River basin of



Ecuador. This distribution highlights clear allopatry within the clade, influenced by the Esmeraldas and Mira river watersheds, which have served as key factors in vertebrate divergence with sympatric species in similar altitudinal bands, approximately at 2000 meters (Hutter, Guayasamin & Wiens, 2013; Mendoza *et al.* 2015, Antonelli *et al.*, 2018; Perrigo *et al.*, 2019; Franco-Mena *et al.* 2023).

Re-examination and re-identification of *Pristimantis verecundus* Lynch & Burrowes type material, confirm the continuity in distribution of *P. verecundus* sensu stricto, with *P. satheri* sp. nov., and *P. robayoi* sp. nov. along the Mira River basin and its tributary micro-basins such San Juan River (Colombia-Ecuador border) and the Guiza River (La Planada Reserve, Colombia).

The presence of the Cerro Golondrinas mountain system within the altitudinal gradient of the Mira River basin, is a key element in the diversification of the *Pristimantis celator* clade, wide altitudinal differences, with sharp rocky walls and deep humid mountain valleys, promoting distinct environments, climate and subsequently speciation in our studied clade, as in other biological groups like orchids (Baquero & Montero 2020; Monteros *et al.*, 2021; Monteros *et al.* 2022). The mountainous landscapes of the Mira River basin act as a vicariance barrier isolating sister species such as *Pristimantis praemortuus* sp. nov. and *Pristimantis broaddus* sp.nov., which exhibit genetic divergences exceeding 3.22% on its western and eastern slopes populations of the species, respectively. Moreover, species on the western side of Cerro Golondrinas show patterns of altitudinal parapatry, with high variation in genetic distances, 10% and 11% between sisters species, showing a clear clinal pattern on the *Pristimantis celator* clade.

Conservation Status. We consider that the four newly described species have highly restricted ranges, closely tied to forested habitats, with distributions not exceeding 150 km². Although *Pristimantis verecundus* is currently listed as Vulnerable (VU B1a (\leq 10) b (iii)); Ortega *et al.*, 2021), our findings suggest an even more restricted range of less than 50 km².

All species in this complex were found outside Ecuador's National System of Protected Areas (SNAP), with distributions confined to private reserves and community-led conservation efforts, such as the Dracula Reserve, Cerro Golondrinas Protected Forest, and the ACUS Chinambí Conservation and Sustainable Use Area.

In Colombia, *Pristimantis verecundus*, *P. satheri* sp. nov., and *P. robayoi* sp. nov. persist in La Planada Reserve. The habitats of these species overlap with areas subject to mining exploration and exploitation (Roy et al., 2018; Ortega-Andrade et al., 2021; Yánez-Muñoz et al., 2020, 2024). Our fieldwork has revealed that these new species, along with *Pristimantis verecundus*, exhibit low relative abundances, with fewer than ten individuals per species collected during each of the nine expeditions conducted in the study area. In contrast, other more abundant species of *Pristimantis*, such as *P. apiculatus*, are three times as common. Given these factors and the ongoing threats to their habitats, these species may warrant classification in a higher extinction risk category (e.g., VU, EN, CR). Until further ecological and population data are available, we suggest assigning the new species as Data Deficient (DD) and re-evaluating the status of *Pristimantis verecundus*.



Conclusions

The study proposes a redefinition of the *Pristimantis verecundus* clade as the *Pristimantis celator* clade, emphasizing the significance of utilizing the oldest available name, *Pristimantis celator* (Lynch, 1976), for this group. This reorganization is consistent with phylogenetic evidence and clarifies the taxonomic status of species within the clade, which is now placed within the broader *Pristimantis myersi* species group under the subgenus *Trachyphrynus*.

The phylogenetic relationships and species delimitation of this study have identified and formally described four new species within the *Pristimantis celator* clade. These descriptions expand the known diversity within the clade from 10 to 14 species, underscoring the clade's cryptic diversity and the importance of thorough phylogenetic analyses for species delimitation.

Although the presence of a polytomy among three well-supported clades within the *Pristimantis myersi* species group, the study offers substantial evidence in support of the clade structure, particularly within the *Pristimantis celator* clade. The polytomy, likely influenced by incomplete genetic data for some species, does not detract from the evidence for the distinctiveness and evolutionary relationships among these groups.

The highly cryptic diversity observed within the *Pristimantis celator* clade can be attributed to the unique orogenic processes and the intricate geological and climatic conditions of the extreme northwestern foothills of the Andes in Ecuador and southern Colombia, along with their associated watersheds. This underscores the clade's endemic nature and highlights the critical need for targeted conservation efforts. The study's findings enhance our understanding of the biogeographic patterns that influence species diversity in these regions, emphasizing the importance of preserving these habitats.

Acknowledgments

We thank the Principal Investigators of the "Biodiversity Conservation in the Mira and Mataje River Basins" project, Paul A. Baker (Duke University) and Jorge Gómez (Beyond One & SDSN Andes) for their support and coordination with the John D. & Catherine T. MacArthur Foundation, without which this work would not have been possible. We thank Sandra Galeano and Christian Venegas-Valencia from the Instituto de Investigación de Recursos Biológicos Alexander von Humboldt, for access to the type collections and for sending important high-resolution photographic material. CRP, JRP, MAU and MYM are grateful for the facilities provided by Diego F. Cisneros-Heredia at the Museo de Zoología, Universidad San Francisco de Quito (ZSFQ). MYM, JCC, MAU, CPV and GLC tanks to Diego Inclan L., Francisco Prieto A., Pablo Sánchez, Jorge Brito M., Cesar Garzón S. and Maurico Herrera Madrid of INABIO for or their support during the development of the project and critical discussions. We thank the collaboration during field work and collections by: Mateo A. Vega-Yánez, Daniel Padilla, Klever Jiménez and Rafael Mena (San Jacinto de Chinambí and Maldonado in 2019); Carlos Castro-Muñoz, Hugo Canchagua and Joseu Canchagua (Cabañas El Pailón, Bosque Protector Golondrinas in 2023); Jaqui Curay,



1116 Rocío Manovandas, Rubí García, Jorge Brito, Glenda Pozo, Jordi Salazar, Fausto Recalde, 1117 Gabriela Puetate, Sara Chingal, Callie Broaddus, Pearson McGovern, Carlos Ríos, Ross Mayner, Jaime Culebras, Natalia Espinoza, Daniel Valencia, Marco Monteros, Andy Better, Mauricio 1118 Herrera-Madrid and the "Dracula's Rangers" of Ecominga Foundation: Hector Yela, Milton 1119 Canticuz, Jeovany Guerra, Rolando Peña, Nilo Ortiz, David Yela (Reserva Dracula from 2015 to 1120 2023). To Lou Jost of Fundación Ecominga for all his contingent and support for the data collection 1121 1122 in Reserva Dracula. To Justin Sather, who motivated much of this research and was the trigger to deepen our investigation. To Callie Broaddus for all her affection in the pleasant and unforgettable 1123 1124 field days and her wonderful photographic work in these last 6 years. To Javier "Capitán" Robayo 1125 for all the confidence and above all for the fun motivations during the field days. To the anonymous 1126 reviewers for their valuable contributions to the manuscript. Thanks for their valuable photographic contributions to: Santiago R. Ron (BioWeb-OCAZ), Jaime Culebras (Wildelife 1127 1128 Tours), Mateo Vega-Yánez (INABIO), Christian Venegas-Valencias and Sandra Galeano (IvH). A special thanks from MYM to Mauro, Alejandra, Joaquín and Julieta, for their constant patience 1129 1130 and love during the field days.

1131

11321133

1134 References

- Antonelli A, Kissling WD, Flantua SG, Bermúdez MA, Mulch A, Muellner-Riehl AN, Hoorn C. (2018). Geological and climatic influences on mountain biodiversity. *Nature Geoscience* 1137 11(10): 718-725 DOI 10.1038/s41561-018-0236-z.
- Baquero LE & Monteros MF. 2020. A new tall and exceptional species of Lepanthes from
 North-West Ecuador (Orchidaceae: Pleurothallidinae). *Lankesteriana*. 20 (3):331-338
 DOI 10.15517/lank.v20i3.44602.
- Beaupre SJ, Jacobson ER, Lillywhite HB, Zamudio K. (2004). *Guidelines for use of live* amphibians and reptiles in field and laboratory research. Lawrence: American Society of
 Ichthyologists and Herpetologists, 43.
- Bejarano-Muñoz P, Ron SR, Navarrete MJ, Yánez-Muñoz MH. (2022). Dos nuevas especies del grupo *Pristimantis boulengeri* (Anura: Strabomantidae) de la cuenca alta del río Napo, Ecuador. *Cuadernos de Herpetología* 36(2):125-154 DOI 10.31017/CdH.2022.(2020-1147) 103).
- Bickford D, Lohman DJ, Sodhi NS, Ng PK, Meier R, Winker K, Das I. (2007). Cryptic species as a window on diversity and conservation. *Trends in ecology & evolution* 22(3):148-155 DOI 10.1016/j.tree.2006.11.004.
- Brito J, Koch C, Percequillo AR, Tinoco N, Weksler M, Pinto CM, Pardiñas UFJ. 2020. A newgenus of oryzomyine rodents (Cricetidae, Sigmodontinae) with three new species from montanecloud forests, western Andean cordillera of Colombia and Ecuador. *PeerJ* 8(2):e10247 DOI 10.7717/peerj.10247.
- 1155 Carrión-Olmedo JC. 2024. juliocesarcaol/NGS run: v1.0.1. DOI 10.5281/zenodo.12802273.



- 1156 Chakrabarty P, Warren M, Page LM, Baldwin CC. (2013). GenSeq: an updated nomenclature 1157 and ranking for genetic sequences from type and non-type sources. *ZooKeys* (346):29-41 1158 DOI 10.3897/zookeys.346.5753.
- 1159 Chan KO, Hertwig ST, Neokleous DN, Flury JM, Brown RM. (2022). Widely used, short 16S
 1160 rRNA mitochondrial gene fragments yield poor and erratic results in phylogenetic
 1161 estimation and species delimitation of amphibians. *BMC Ecology and Evolution* 22(1):37
 1162 DOI 10.1186/s12862-022-01994-y.
- Duellman WE. 1979. The herpetofauna of the Andes: patterns of distribution, origins, differentiation, and present communities. In: Duellman WE, ed. *The South American Herpetofauna: Its Origin, Evolution, and Dispersal*. Lawrence: Monographs of the Museum of Natural History. The University of Kansas, 371–459.
- Duellman WE, Lehr E. 2009. Terrestrial-breeding Frogs (Strabomantidae) in Peru. Natur und
 Tier Verlag, Münster, 382 pp.
- Franco-Mena D, Guayasamin JM, Andrade-Brito D, Yánez-Muñoz MH, Rojas-Runjaic FJ.

 (2023). Unveiling the evolutionary relationships and the high cryptic diversity in Andean rainfrogs (Craugastoridae: *Pristimantis myersi* group). *PeerJ* 11(4): e14715 DOI 10.7717/peerj.14715.
- Frost DR. 2023. Amphibian species of the world: an online reference. Version 6.1 (23 of may 2024). New York, USA: American Museum of Natural History. DOI 10.5531/db.vz.0001.
- Gonzalez BC, Martínez A, Borda E, Iliffe TM, Eibye-Jacobsen D, Worsaae K. (2018).
 Phylogeny and systematics of Aphroditiformia. *Cladistics* 34(3):225-259 DOI 10.1111/cla.12202.
- Guayasamin JM, Krynak T, Krynak K, Culebras J, Hutter CR. (2015). Phenotypic plasticity raises questions for taxonomically important traits: a remarkable new Andean rainfrog (*Pristimantis*) with the ability to change skin texture. *Zoological Journal of the Linnean Society* 173(4):913-928 DOI 10.1111/zoj.12222.
- Köhler G. 2012. Color Catalogue for Field Biologists. Herpeton, Offenbach. ISBN 9783936180404.Offenbach. Germany.
- Guindon S, Dufayard JF, Lefort V, Anisimova M, Hordijk W, Gascuel O. 2010. New algorithms and methods to estimate maximum-likelihood phylogenies: assessing the performance of PhyML 3.0. *Systematic biology* 59(3):307-321 DOI 10.1093/sysbio/syq010.
- Hay JM, Ruvinsky I, Hedges SB, Maxson LR. 1995. Phylogenetic relationships of amphibian families inferred from DNA sequences of mitochondrial 12S and 16S ribosomal RNA genes. *Molecular biology and evolution* 12(5):928-937 DOI 10.1093/oxfordjournals.molbev.a040270.
- Heinicke MP, Duellman WE, Hedges SB. 2007. Major Caribbean and Central American frog
 faunas originated by ancient oceanic dispersal. *Proceedings of the National Academy of Sciences* 104:10092–10097. DOI 10.1073/pnas.0611051104.



- Hedges SB, Duellman WE, Heinicke MP. 2008. New World direct-developing frogs (Anura:
- 1195 Terrarana): molecular phylogeny, classification, biogeography, and conservation.
- 1196 *Zootaxa* 1737:1–182 DOI 10.11646/zootaxa.1737.1.1.
- Hammer Ø, Harper D, Ryan PD. 2001. Past: paleontological statistics software package foreducation and data analysis. Paleontologia Electron 4(1):9.
- Hutter, CR, Guayasamin JM, Wiens JJ. 2013. Explaining Andean megadiversity: The
 evolutionary and ecological causes of glassfrog elevational richness patterns. *Ecology Letters* 16(9):1135-1144 DOI 10.1111/ele.12148.
- Jetz W, Pyron RA. 2018. The interplay of past diversification and evolutionary isolation with present imperilment across the amphibian tree of life. *Nature Ecology and Evolution* (2)850–858 DOI 10.1038/s41559-018-0515-5.
- Katoh K, Standley DM. 2013. MAFFT Multiple Sequence Alignment Software Version 7:
 Improvements in Performance and Usability. *Molecular Biology and Evolution* 30:772–780 DOI 10.1093/molbev/mst010.
- Lynch JD. 1976. New species of frogs (Leptodactylidae: *Eleuhterdactylus*) from the Pacific
 cersant of Ecuador. *Occasional Papers of the Museum of Natural History, University of Kansas* 55: 1–33.
- Lynch JD, Burrowes PA. (1990). The frogs of the genus *Eleutherodactylus* (family
 Leptodactylidae) at the La Planada Reserve in southwestern Colombia with descriptions
 of eight new species. *Occasional Papers of the Museum of Natural History, University of Kansas* 136:1–31.
- Lynch JD, Duellman WE. 1997. Frogs of the genus *Eleutherodactylus* in Western Ecuador:
 systematics, ecology, and biogeography. *The University of Kansas, Natural History Museum, Special Publication* 23: 1-236.
- Mendoza AM, Ospina OE, Cardenas-Henao H, García-R JC. 2015. A likelihood inference of
 historical biogeography in the world's most diverse terrestrial vertebrate genus:
 Diversification of direct-developing frogs (Craugastoridae: *Pristimantis*) across the
 Neotropics. *Molecular Phylogenetics and Evolution* 1055-7903. DOI

1222 10.1016/j.ympev.2015.02.001.

- Ministerio del Ambiente del Ecuador (MAE). 2013. Sistema de Clasificación de los Ecosistemas
 del Ecuador Continental. Subsecretaríade Patrimonio Natural. Quito.
- Mahony S, Kamei RG, Brown RM, Chan KO. 2024. Unnecessary splitting of genus-level clades
 reduces taxonomic stability in amphibians. *Vertebrate Zoology* 74:249–277. DOI
 10.3897/vz.74.e114285.
- Moen DS, Wiens JJ. 2009. Phylogenetic evidence for competitively driven divergence: Bodysize evolution in caribbean treefrogs (Hylidae: *Osteopilus*). *Evolution* 63:195–214. DOI 10.1111/j.1558-5646.2008.00538.x.
- Monteros MF, Baquero LE & Vieira-Uribe S. 2021. A new Pseudolepanthes (Pleurothallidinae: Orchidaceae) from Northwest Ecuador. *Lankesteriana* 21(1):5-10 DOI
- 1233 10.15517/lank.v21i1.45877.



1248

- Monteros MF, Restrepo E & Baquero LE. 2022. *Platystele finleyae* (Pleurothallidinae), a new
 species from northwestern Ecuador. *Lankesteriana* 22(1):63-72. DOI
 10.15517/lank.v22i1.50869.
- 1237 Ortega-Andrade HM, Rodes Blanco M, Cisneros-Heredia DF, Guerra Arévalo N, López de 1238 Vargas-Machuca KG, Sánchez-Nivicela JC. Armijos-Ojeda D, Cáceres Andrade JF, 1239 Reyes-Puig C, Quezada Riera A, Székely P, Rojas Soto OR, Székely D, Guayasamin JM, Siavichay Pesántez FR, Amador L, Betancourt R, Ramírez-Jaramillo S, Timbe-Borja B, 1240 Gómez Laporta M, Webster Bernal JF, Oyagata Cachimuel LA, Chávez Jácome D, Posse 1241 1242 V, Valle-Piñuela C, Padilla Jiménez D, Reyes-Puig JP, Terán-Valdez A, Coloma LA, 1243 Pérez Lara MB, Carvajal-Endara S, Urgilés M, Yánez Muñoz MH. (2021). Red List 1244 assessment of amphibian species of Ecuador: A multidimensional approach for their
- 1245 conservation. *PloS one* 16(5):e0251027 DOI 10.1371/journal.pone.0251027.
 1246 Ortega JA, Brito J, Ron SR. 2022. Six new species of *Pristimantis* (Anura: Strabomantidae) from
 1247 Llanganates National Park and Sangay National Park in Amazonian cloud forests of
- Padial JM, Grant T, Frost DR. 2014. Molecular systematics of terraranas (Anura:
 Brachycephaloidea) with an assessment of the effects of alignment and optimality
 criteria. *Zootaxa* 3825(1):1–132 DOI 10.11646/zootaxa.3825.1.1.

Ecuador. *PeerJ* 10:e13761 DOI 10.7717/peerj.13761.

- Perrigo A, Hoorn C, Antonelli A. 2019. Whymountains matter for biodiversity. *Jornual of Biogeography* 47:315–325 DOI 10.1111/jbi.13731.
- Pinto-Sánchez NM, Ibáñez R, Madriñán S, Sanhur OI, Bermingham E, Crawford AJ. 2015. The
 Great American Biotic Interchange in frogs: Multiple and early colonization of Central
 America by the South American genus *Pristimantis* (Anura: Craugastoridae). *Molecular Phylogenetics and Evolution* 62:954–972 DOI 10.1016/j.ympev.2011.11.022.
- Portik DM, Streicher JW, Blackburn DC, Moen DS, Hutter CR, Wiens JJ. 2023. Redefining Possible: Combining Phylogenomic and Supersparse Data in Frogs. *Molecular Biology and Evolution* 40:msad109 DOI 10.1093/molbev/msad109.
- Reyes-Puig C, Wake DB, Kotharambath R, Streicher JW, Koch C, Cisneros-Heredia DF, Yánez-Muñoz MH, Ron S. 2020a. Two extremely rare new species of fossorial salamanders of the genus *Oedipina* (Plethodontidae) from northwestern Ecuador. *PeerJ* 8:e9934 DOI 10.7717/peerj.9934.
- Reyes-Puig C, Yánez-Muñoz MH, Ortega JA, Ron SR. (2020b). Relaciones filogenéticas del subgénero *Hypodictyon* (Anura: Strabomantidae: *Pristimantis*) con la descripción de tres especies nuevas de la región del Chocó. *Revista Mexicana de Biodiversidad* 91.913013 DOI 10.22201/ib.20078706e.2020.91.3013.
- Reyes-Puig C, Mancero E. (2022). Beyond the species name: an analysis of publication trends and biases in taxonomic descriptions of rainfrogs (Amphibia, Strabomantidae, *Pristimantis*). ZooKeys, 1134, 73. DOI 10.3897/zookeys.1134.91348
- 1272 Reyes-Puig JP, Yánez-Muñoz MH, Libke Z, Vinueza P, Carrión-Olmedo JC. (2024).
- Phylogenetic diversity of the *Pristimantis anaiae* species group, with a description of a



1274 new species of *Pristimantis* (Anura, Strabomantidae) from Cerro Candelaria, 1275 Tungurahua, Ecuador. Evolutionary Systematics 8:101-118. DOI 1276 10.3897/evolsyst.8.118855. 1277 Rivera-Correa M y Daza JM. (2016). Molecular phylogenetics of the *Pristimantis lacrimosus* 1278 species group (Anura: Craugastoridae) with the description of a new species from 1279 Colombia. Acta Herpetologica 11(1):31-45 DOI 10.13128/Acta Herpetol-16434 Rueda JV, Castro F y Cortez C. 2006. Técnicas para el inventario y muestreo de anfibios: Una 1280 1281 compilación. Pp: 135-171. In: Angulo A., J. V. Rueda-Almonacid, J. V. Rodríguez-1282 Mahecha y E. La Marca (Eds.). Técnicas de inventario y monitoreo para los anfibios de 1283 la región tropical andina. Conservación Internacional. Serie Manuales de Campo Nº 2. 1284 Panamericana Formas e Impresos S.A., Bogotá D.C. 298 pp. Ron SR, Merino A y Ortiz D. 2024. Anfibios del Ecuador. Museo de Zoología, Pontificia 1285 Universidad Católica del Ecuador.2024 [13/01/24]. Version 2024.0.:[Available from: 1286 1287 https://bioweb.bio/faunaweb/amphibiaweb. 1288 Roy BA, Zorrilla M, Endara L, Thomas DC, Vandegrift R, Rubenstein JM, Read M. (2018). New mining concessions could severely decrease biodiversity and ecosystem services in 1289 1290 Ecuador. Tropical Conservation Science 11:1940082918780427 DOI 10.1177/1940082918780427. 1291 1292 Sahlin K, Lim MCW, Prost S. 2021. NGSpeciesID: DNA barcode and amplicon consensus 1293 generation from long-read sequencing data. Ecology and Evolution 11:1392–1398. DOI 1294 10.1002/ece3.7146. 1295 Santander T, Freile JF, & Loor-Vela S. 2009. Ecuador. Pág. 187 –196 In: C. Devenish, D. F. 1296 Díaz Fernández, R. P. Clay, I. Davidson & I. Yépez Zabala (Eds.). Important Bird Areas 1297 Americas - Priority sites for biodiversity conservation. Quito, Ecuador: BirdLife 1298 International (BirdLife Conservation Series No. 16). Tamura K, Stecher G, Kumar S. 2021. MEGA11: Molecular Evolutionary Genetics Analysis 1299 1300 Version 11, Molecular Biology and Evolution 38(7):3022–3027. DOI 1301 10.1093/molbey/msab120. Trifinopoulos J, Nguyen LT, von Haeseler A, Minh BO. 2016. W-IO-TREE: a fast online 1302 1303 phylogenetic tool for maximum likelihood analysis. *Nucleic acids research* 44(W1), 1304 W232-W235 DOI 10.1093/nar/gkw256. Vasconcelos TS, Da Silva FR, Dos Santos TG, Prado VH, Provete DB. (2019). Biogeographic 1305 patterns of South American anurans. Springer DOI 10.1007/978-3-030-26296-9. 1306 Vasiljevic N, Lim M, Humble E, Seah A, Kratzer A, Morf NV, Ogden R. (2021). Developmental 1307 validation of Oxford Nanopore Technology MinION sequence data and the NGSpeciesID 1308 1309 bioinformatic pipeline for forensic genetic species identification. Forensic Science 1310 International: Genetics 53:102493 DOI 10.1016/j.fsigen.2021.102493. 1311 Vences M, Guayasamin JM, Miralles A, De La Riva I. 2013. To name or not to name: Criteria to 1312 promote economy of change in Linnaean classification schemes. Zootaxa 3636: 201–244. 1313 DOI 10.11646/zootaxa.3636.2.1.

1314 Waddell EH, Crotti M, Lougheed SC, Cannatella DC, Elmer KR. 2018. Hierarchies of 1315 evolutionary radiation in the world's most species rich vertebrate group, the Neotropical Pristimantis leaf litter frogs. Systematics and Biodiversity 16(8):807-819 DOI 1316 1317 10.1080/14772000.2018.1503202. 1318 Wiens JJ, Fetzner Jr, JW, Parkinson CL, Reeder TW. (2005). Hylid frog phylogeny and sampling 1319 strategies for speciose clades. Systematic biology 54(5):778-807 DOI 1320 0.1080/10635150500234625. Yánez-Muñoz MH, Reyes-Puig C, Reyes-Puig JP, Velasco JA, Ayala-Varela F, Torres-Carvajal 1321 1322 O. (2018). A new cryptic species of *Anolis* lizard from northwestern South America 1323 (Iguanidae, Dactyloinae). ZooKevs (794):135 DOI 10.3897/zookevs.794.26936. 1324 Yánez-Muñoz MH, Meza-Ramos PA, Cisneros-Heredia DF, Reves-Puig JP. 2010. Descripción 1325 de tres nuevas especies de ranas del género *Pristimantis* (Anura: Terrarana: 1326 Strabomantidae) de los bosques nublados del Distrito Metropolitano de Quito, Ecuador. 1327 ACI Avances en Ciencias e Ingenierías 2(3) DOI 10.18272/aci.v2i3.40. 1328 Yánez-Muñoz M H, Batallas D, Meza-Ramos PA, Oyagata LA, Padilla D, Paucar C, Ramírez S, 1329 Reyes-Puig JP, Rodríguez MA, Urgilés-Merchán MA, Vega-Yánez M. 2020. Anfibios en los Ecosistemas Andino-Tropicales de la Provincia del Carchi. Serie de Publicaciones 1330 del Instituto Nacional de Biodiversidad. Monografía N° 14:1-400. INABIO – GADPC 1331 1332 Yánez-Muñoz MH, Reyes-Puig JP, Batallas-Revelo D, Broaddus C, Urgilés-Merchán M, Cisneros-Heredia DF, Guayasamin JM. 2021. A new Andean treefrog (Amphibia: 1333 1334 Hyloscirtus bogotensis group) from Ecuador: an example of community involvement for 1335 conservation. *PeerJ* 9:e11914. DOI 10.7717/peerj.11914. 1336 Yánez-Muñoz MH, Torres-Carvajal O, Reyes-Puig JP, Urgiles-Merchán MA, Koch C. (2021). A 1337 new and very spiny lizard (Gymnophthalmidae: Echinosaura) from the Andes in 1338 northwestern Ecuador. PeerJ 9:e12523 DOI 10.7717/peerj.12523 Yánez-Muñoz Brito J, Román RR, Juranny M, Astorquiza A, Baca E, Baker PA, Bejarano-1339 1340 Muñoz P, Eric Y. Cuesta R, Freire E, Garzón C, Gómez-Paredes J, Klinger W, Lagos LE, 1341 MedinaW, Mena-Valenzuela P, Mosquera LJ, Mosquera RS, Murillo Y, Yiscar D. Murillo A, Nagle E, Narváez G, Pimm S, Proaño C, Prieto F, Ouezada Z, Ramírez G, 1342 Rengifo R, Rentería LE, Urgilés-Merchán MA, Vargas L, Valdospinos C, Valolyes Z, 1343 1344 Inclán DJ. 2024. The Tropical Andes Biodiversity Hotspot: A Comprehensive Dataset for the Mira-Mataje Binational Basins. Scientific Data 782(2024). DOI 10.1038/s41597-024-1345 1346 03463-1. 1347 Zou F, Bhuiyan MA, Crovella T, Paiano A. (2024). Analyzing the borderlands: a regional report on the Colombia-Ecuador border on political, economic, social, legal, and environment 1348 1349 aspects. International Migration Review 58(2):881-897 DOI 1350 10.1177/0197918322114901.



Table 1(on next page)

Table 1.

List of localities sampled in the Mira River Basin in Ecuador for this research.



1 TABLES

2 **Table 1.** List of localities sampled in the Mira River Basin in Ecuador for this research.

N°	Locality	Collectors	Geographic coordinates	Elevation in meters above sea	Collection date
1	Reserva Drácula, Sector Cerro Oscuro	Mario H. Yánez- Muñoz, Juan P. Reyes-Puig & Jorge Brito M.	0.898426 - 78.207942	level 1600	From: 2015-07- 18 to: 2015-07- 22
2	Reserva Drácula, Sector El Pailón	Mario H. Yánez- Muñoz & Juan P. Reyes-Puig	1.0125630 - 78.24620	1450	From: 2017-11- 08 to: 2017-11- 12 From: 2018- 04-23 to: 2018- 04-28
3	San Jacinto de Chinambí	Mario H. Yánez- Muñoz, Mateo Vega Yánez & Daniel Padilla	0.860927 - 78.272364	2600	From: 2019-06-8 to: 2019-06-15
4	Sector La Esperanza	Mario H. Yánez- Muñoz, Juan P. Reyes-Puig, Evelyn Gabriela Lagla Chimba, & Miguel Urgiles	0.937383 -78.2425	1670	From: 2021-03- 24 To 2021-03- 30
5	Bosque Protector Cerro Golondrinas, Sector Cañas el Pailón	Miguel Andrés Urgilés Merchán, Christian Paucar Veintimilla	0.82377 -78.09519	2510	From: 2023-07- 25 To: 2023-08- 01
6	Reserva Drácula, Base del Cerro	Juan P. Reyes-Puig	0.85784 -78.19729	2093	From: 2023-06- 18 To: 2023-07- 07
7	Golondrinas Reserva Drácula, Sector Cerro	Ross Maynard	0.87102 -78.2069	2221	From: 2021-08- 15 To: 2023-07- 08
8	Negro Reserva Drácula, Base del Cerro Golondrinas	Julio C. Carrión, Pearson Mcgoovern, Callie Broadus	0.88413 -78.2077	1962	From: 2021-08- 03 to: 2021-08- 12
9	Reserva Drácula, Base del	Evelyn Gabriela Lagla Chimba & Julio C. Carrión O.	0.86638 - 78.202444	2277	From: 2022-08- 03 to: 2022-08- 12





Cerro Golondrinas

10 Reserva Mario H. Yánez-Drácula, Muñoz, Miguel Sector Los Andrés Urgilés Olivos Merchán, Christian (Bloque 20) Paucar Veintimilla, Carlos Ríos 0.83645 -78.24127

2335 From: 2023-12-05 to: 2023-12-

14

3



Table 2(on next page)

Table 2.

Morphometric characters of the news species and *Pristimantis vercundus*.

Table 2. Morphometric characters of the news species and *Pristimantis vercundus*.

	P sather	i sn nov	P. broaddus sp. nov.	P praemor	tuus sp. nov.	P robava	oi sp. nov.	P. verec	undus
	P. satheri sp. nov. Females Males		Females	Females	Males	Females	Males	Females	Males
Character	n = 2	n = 2	n = 8	n = 3	n = 5	n = 7	n = 3	n = 4	n = 3
SVL	22.08-23.74 (2) 22.91 ± 1.17	19.73-19.79 (2) 19.76 ± 0.04	16.81-18.42 (8) 17.62 ± 1.14	17.03-17.68 (3) 17.35 ± 0.46	$12.46-17.4 (5) 14.93 \pm 3.49$	21.78-29.05 (7) 25.42 ± 5.14	18.08-23.32 (3) 20.7 ± 3.71	18.57-22.84 (4) 20.71 ± 3.02	17.56- 19.24 (3) 18.4 ± 1.19
HW	$7.74-8.51$ (2) 8.13 ± 0.54	6.95-6.99 (2) 6.97 ± 0.03	$5.28-6.22$ (8) 5.75 ± 0.66	5.99-6.16(3) 6.16 ± 0.09	5.13-5.99(5) 5.56 ± 0.61	$7.68-9.81$ (7) 8.75 ± 1.51	$6.31-8.61$ (3) 7.46 ± 1.63	7.15-8.76 (4) 7.96 ± 1.14	6.26-7.3(3) 6.78 ± 0.74
HL	8.76-9.23 (2) 9 ± 0.33	7.6-7.62 (2) 7.61 ± 0.01	5.62-6.26 (8) 5.94 ± 0.45	5.26-6.2(3) 5.66 ± 0.57	$4.43-5.6$ (5) 5.02 ± 0.83	6.7-9.51 (7) 8.11 ± 1.99	5.3-7.42(3) 6.36 ± 1.5	5.9-7.35(4) 6.63 ± 1.03	5.12-6.52 (3) 5.82 ± 0.99
EN	$2.15-2.65$ (2) 2.4 ± 0.35	$1.99-2.1 (2) 2.05 \pm 0.08$	$1.58-2.75$ (8) 2.17 ± 0.83	1.71-1.86(3) 1.73 ± 0.08	1.31-1.97 (5) 1.64 ± 0.47	2.19-3.17 (7) 2.68 ± 0.69	$1.9-2.61 (3) 2.26 \pm 0.5$	$1.72-2.4 (4) 2.06 \pm 0.48$	1.53-2.04 (3) 1.79 ± 0.36
IND	1.77-1.91 (2) 1.84 ± 0.1	$1.56-1.6 (2) 1.58 \pm 0.03$	1.64-1.91 (8) 1.78 ± 0.19	1.74-1.75(3) 1.76 ± 0.03	$1.34-1.7 (5) 1.52 \pm 0.25$	$1.73-2.28 (7) 2.01 \pm 0.39$	$1.69-1.84(3)$ 1.77 ± 0.11	1.69-2.1 (4) 1.9 ± 0.29	1.63-1.87 (3) 1.75 ± 0.17
IOD	$2.6-2.62$ (2) 2.61 ± 0.01	$2.12-2.21$ (2) 2.17 ± 0.06	$1.69-2.43$ (8) 2.06 ± 0.52	1.79-2.15(3) 1.86 ± 0.09	1.6-1.95(5) 1.78 ± 0.25	2.23-2.96 (7) 2.6 ± 0.52	$1.84-2.5 (3) 2.17 \pm 0.47$	2-2.42(4) 2.21 ± 0.3	1.93-2.19 (3) 2.06 ± 0.18
EW	1.56-2 (2) 1.78 ± 0.31	$1.39-1.4 (2) 1.4 \pm 0.01$	$1.2-1.52 (8) 1.36 \pm 0.23$	1.36-1.47(3) 1.43 ± 0.09	1.12-1.75 (5) 1.44 ± 0.45	1.79-3.04 (7) 2.42 ± 0.88	1.67-2.15(3) 1.91 ± 0.34	1.38-2.32 (4) 1.85 ± 0.66	1.42-1.77 (3) 1.6 ± 0.25
TD	0.97-1.06 (2) 1.02 ± 0.06	0.9 - 0.95 (2) 0.93 ± 0.04	0.88-1.11(8) 1 ± 0.16	0.89 - 0.95(3) 1.02 ± 0.12	0.8-1.09(5) 0.95 ± 0.21	0.7-1.12 (7) 0.91 ± 0.3	0.76-1.22(3) 0.99 ± 0.33	0.69 - 0.91 (4) 0.8 ± 0.16	$0.77-0.98$ $(3) 0.88 \pm 0.15$
ED	2.83-3.14 (2) 2.99 ± 0.22	2.5-2.53 (2) 2.52 ± 0.02	$1.97-2.48$ (8) 2.23 ± 0.36	$1.72-2.2 (3) 2.06 \pm 0.48$	1.79-2.15 (5) 1.97 ± 0.25	3.09-3.5 (7) 3.3 ± 0.29	$2.83-3.26$ (3) 3.05 ± 0.3	2.43-2.77 (4) 2.6 ± 0.24	1.87-2.66 (3) 2.27 ± 0.56
TL	11.05-11.63 (2) 11.34 ± 0.41	$9.25-9.8$ (2) 9.53 ± 0.39	7.79-8.44(8) 8.12 ± 0.46	1.5-8.18(3) 5.09 ± 5.07	6.54-8.95(5) 7.75 ± 1.7	10.55-13.76 (7) 12.16 ± 2.27	9.72-13.31 (3) 11.52 ± 2.54	8.88-10.94 (4) 9.91 ± 1.46	8.45-9.6(3) 9.03 ± 0.81

HL	$6.78-7.13$ (2) 6.96 ± 0.25	5.6-5.92 (2) 5.76 ± 0.23	$4.75-5.49$ (8) 5.12 ± 0.52	4.73-4.97(3) 5.05 ± 0.45	4.07-4.65(5) 4.36 ± 0.41	$6.52-8.3$ (7) 7.41 ± 1.26	5.63-7.26(3) 6.45 ± 1.15	$5.23-6.57$ (4) 5.9 ± 0.95	5.5-6.43(3) 5.97 ± 0.66
FL	11.05-11.86 (2) 11.46 ± 0.57	9.5-9.7 (2) 9.6 ± 0.14	$2.12-9.26$ (8) 5.69 ± 5.05	7.99-8.59(3) 8.51 ± 0.73	6.58-7.71(5) 7.15 ± 0.8	10.24-13.47 (7) 11.86 ± 2.28	8.97-10.64 (3) 9.81 ± 1.18	8.55-10.59 (4) 9.57 ± 1.44	8.79-9.9(3) 9.35 ± 0.78
FW	1.08-1.27 (2) 1.18 ± 0.13	$0.88-0.89$ (2) 0.89 ± 0.01	0.54-1.02 (8) 0.78 ± 0.34	0.64-0.85(3) 0.76 ± 0.17	0.59-0.74(5) 0.67 ± 0.11	$1-1.44 (7) 1.22 \pm 0.31$	0.74-1.15(3) 0.95 ± 0.29	0.99-1.38 (4) 1.19 ± 0.28	$0.99-1.16$ (3) 1.08 ± 0.12
TW	0.98-1.04 (2) 1.01 ± 0.04	$0.6-0.64$ (2) 0.62 ± 0.03	0.41 - 0.81 (8) 0.61 ± 0.28	0.51-0.59(3) 0.58 ± 0.04	0.47-0.76 (5) 0.62 ± 0.21	0.95-1.35(7) 1.15 ± 0.28	0.59-1.24(3) 0.92 ± 0.46	0.85-1.23 (4) 1.04 ± 0.27	$0.68-0.76$ $(3) 0.72 \pm 0.06$

²

4

5

Measurements: Snout-vent length (SVL), Head width (HW), Head length (HL), Horizontal eye diameter (ED), Interorbital distance (IOD)Eye-nostril distance (EN), Tympanic length (TD), Internarinal distance (IND), Tibia length (TL), Upper eyelid width, Foot length (FoL), Hand length (HaL), Disc width of finger III (F3D), Disc width of toe IV (T4D).

PeerJ

Table 3(on next page)

Appendix I.

Examined specimens



- 1 Appendix 1. Specimens examined. Pristimantis broaddus (9): Ecuador: Carchi (9): Cabañas El
- 2 Pailón, Bosque Protector Golondrinas DHMECN 19037 (Holotype), DHMECN 19028–19029,
- 3 DHMECN 19031–36. Pristimantis mutabilis (5): Ecuador: Imbabura (5): Lita, DHMECN 11755;
- 4 Concesión Llumiragua DHMECN 13279; Concesión Cascabel ENSA, DHMECN 14796;
- 5 Reserva Manduriacu DHMECN 16433; Reserva comunitaria Junín DHMECN 19479.
- 6 Pristimantis praemortuus (9): Ecuador: Carchi (9): Los Olivos-Bloque 20, Reserva Dracula
- 7 DHMECN 19591(Holotype), DHMECN 19535, DHMECN 19546–47, DHMECN 19557,
- 8 DHMECN 19570, DHMECN 19577, DHMECN 19579; San Jacinto de Chinambí, DHMECN
- 9 14887. Pristimantis robayoi (14): Ecuador: Carchi (13) Base del Golondrinas, Reserva Dracula,
- 10 DHMECN 17894 (Holotype), DHMECN 16567, DHMECN 16573, DHMECN 16575,
- 11 DHMECN 19429; San Jacinto de Chinambí DHMECN 14884, DHMECN14886; Río Cumbe,
- 12 Maldonado DHMECN14947–48, DHMECN 14950, DHMECN 14953, DHMECN14960; La
- 13 Esperanza, Quinshull DHMECN 16150. COLOMBIA (1): Dpto. de Nariño (1): Reserva La
- 14 Planada IAvH-AM-1493. Pristimantis sathreri (7). Ecuador: Carchi (6): San Jacinto de
- 15 Chinambí, DHMECN 14858 (Holotype), DHMECN 14885; Bloque 18, Reserva Dracula,
- DHMECN 16578, DHMECN 16574; Los Olivos-Bloque 20, Reserva Dracula DHMECN 19538;
- 17 Base del Golondrinas, Reserva Dracula, DHMECN 17903. COLOMBIA: Dpto. de Nariño (1):
- 18 Reserva La Planada, IAvH-AM-1492. Pristimantis verecundus: Ecuador: Carchi (9): Reserva
- 19 Dracula, Sector Cerro Negro, DHMECN 15007, DHMECN 15188; Reserva Dracula, sector
- 20 Base del Golondrinas, DHMECN 16568–69; Reserva Dracula, sector Gualpi DHMECN 12597,
- 21 DHMECN 15189, DHMECN 19432–33; Colombia: Dpto. de Nariño (2): Reserva La Planada
- 22 IAvH-AM-1834 (Holotype), IAvH-AM-1457 (Paratype). Pristimantis sp. 3.: Ecuador: Carchi
- 23 (1): Reserva Dracula: Sector El Pailón DHMECN 14006. *Pristimantis* sp. 4.: Ecuador: Carchi
- 24 (2): Reserva Dracula: Sector El Pailón DHMECN 13984, DHMECN 16572. Pristimantis sp. 6.:
- 25 Ecuador: Pichincha (15): Reserva Experimental La Favorita DHMECN 1928, DHMECN 2023;
- 26 Curipogio DHMECN 1927; 5918, 7399–06, 7437–39.



Table 4(on next page)

Appendix

Key of identification for frogs of the *Pristimantis celator* clade.



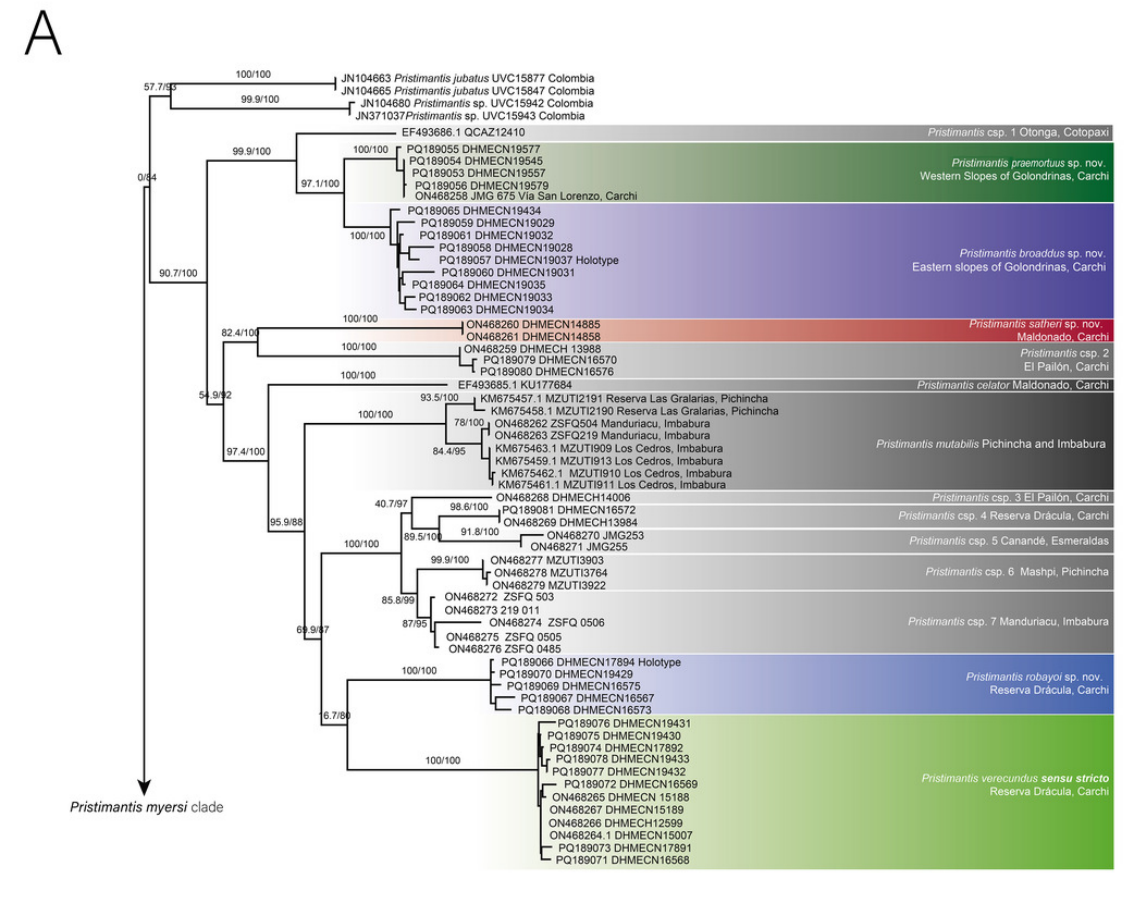
Material supplementary 1.

2	Identification key for frogs of the Pristimantis celator clade.						
3	1a. Large digits, dorsolateral dermal ridges, or glandular folds, conical elongate or subconical tubercles on						
4	eyelid, forearm and heel						
5	1b. Short digits, without glandular folds or dorsolateral dermal ridges, without tubercles on eyelid, forearm						
6	or heel						
7	2a. Digital pads of toes narrow, about the width of the digit or 1.5X the size of the						
8	digit3						
9	2b. Digital pads of toes expanded, wider than the digit, 2X or more the width of the digit4						
10	3a. Tympanic annulus and lateral fringes on fingers are weekly defined						
11	3.b Tympanic annulus clearly defined and lateral fringes, strongly crenulated mainly in finger IV						
12	P. praemortuus						
13	4a. Dorsal lateral folds formed by dermal ridges, with large conical tubercles on the upper eyelid and heel.						
14	5						
15	4b. Dorsolateral glandular fold and tibial gland, with small subconical tubercles on eyelid and heel						
16	P. satheri						
17	5a. Dorsolateral folds extending posteriorly beyond the sacrum						
18	5b.Dorsolateral folds short, only reaching the sacrum, at the anterior border of						
19	ilium						
20	5c. Dorsolateral fold extending to the sacrum, with two distinct black subconical scapular						
21	tubercle						
22							

Figure 1.

Phylogeny of *Pristimantis celator* clade. (A) Maximum Likelihood clade credibility tree obtained from 3955 bp long for 53 individuals; (B) Relationship of *Pristimantis celator* clade to *P. myersi* species group and its sister clades; (C) Phylogenetic position of the *Pristimantis celator* clade and sister clades within the genus *Pristimantis*, from 325 individuals.





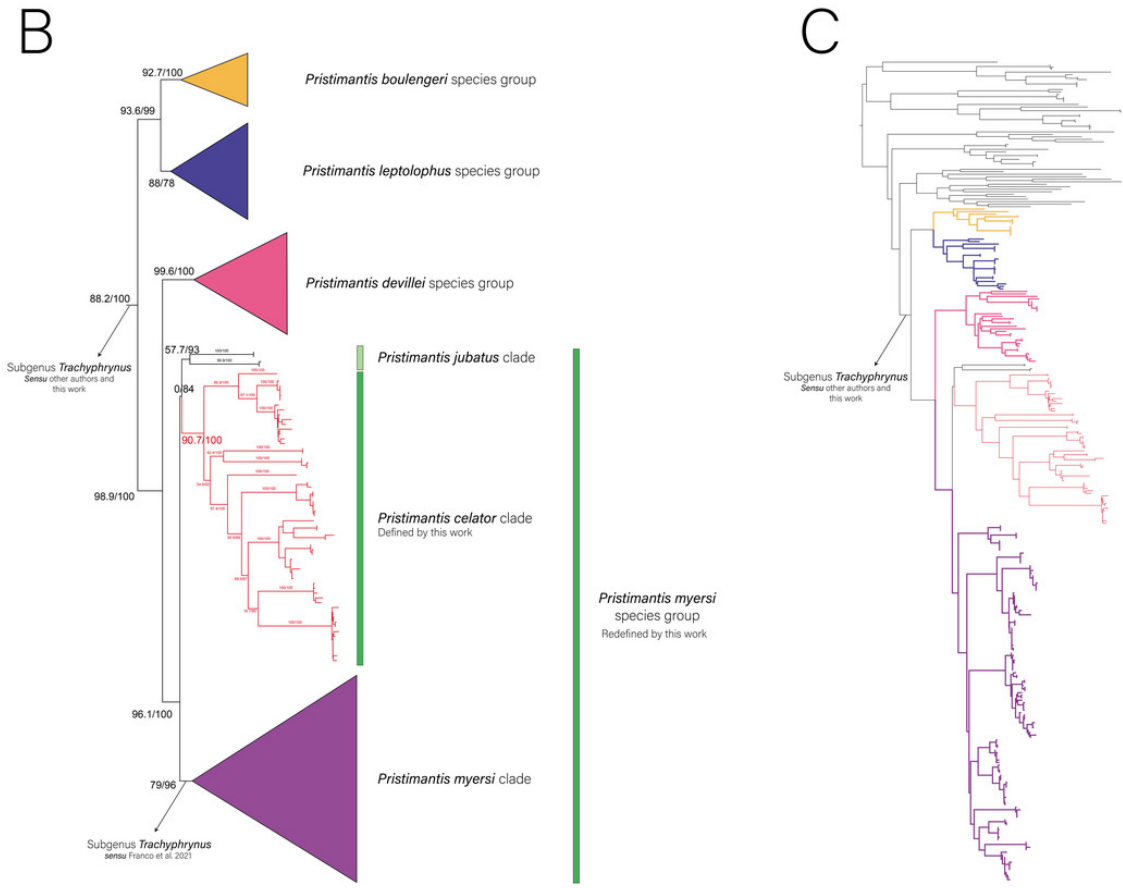


Figure 2.

Some species of *Pristimantis celator* clade. (A) *P. celator* QCAZ66230, Maldonado, Carchi; (B) *P. verecundus* DHMECN 12599, Cerro Oscuro, Reserva Dracula, Carchi; (C) *P. mutabilis*, QCAZ 76813, Los Cedros, Imbabura; (D) *P. broaddus* sp. nov., DHMECN 19037, Holotype, Cabañas el Pailón, Bosque Protector Cerro Golondrinas; (e) *P. praemortuus* sp. nov., DHMECN 19557, Holotipo, Bloque 20, Reserva Dracula, Carchi; (F) *P. robayoi* sp. nov. DHMECN 17894, holotype, Cerro Negro, Reserva Dracula, Carchi; (G) *P. satheri* sp. nov. DHMECN 14858, holotype, Chinambí, Carchi; (H) *P.* c.sp.2 DHMECN 16570, El Pailón, Reserva Dracula. Carchi; (I) *P.* c.sp.7, no collected specimen, Reserva Manduriacu, Imbabura; (J) *P.* c.sp.7, no colectado, Reserva Manduriacu, Imbabura; (K) *P.* c.sp.5, no collected specimen, Reserva Taira, Esmeraldas. Not scale. Photographs by Mario H. Yánez Muñoz (B, J), Christian Paucar V. (D, E), Julio C. Carrión (F), Santiago R. Ron (A,C), Mateo Vega-Yánez (G), Jaime Culebras (H, I, J).



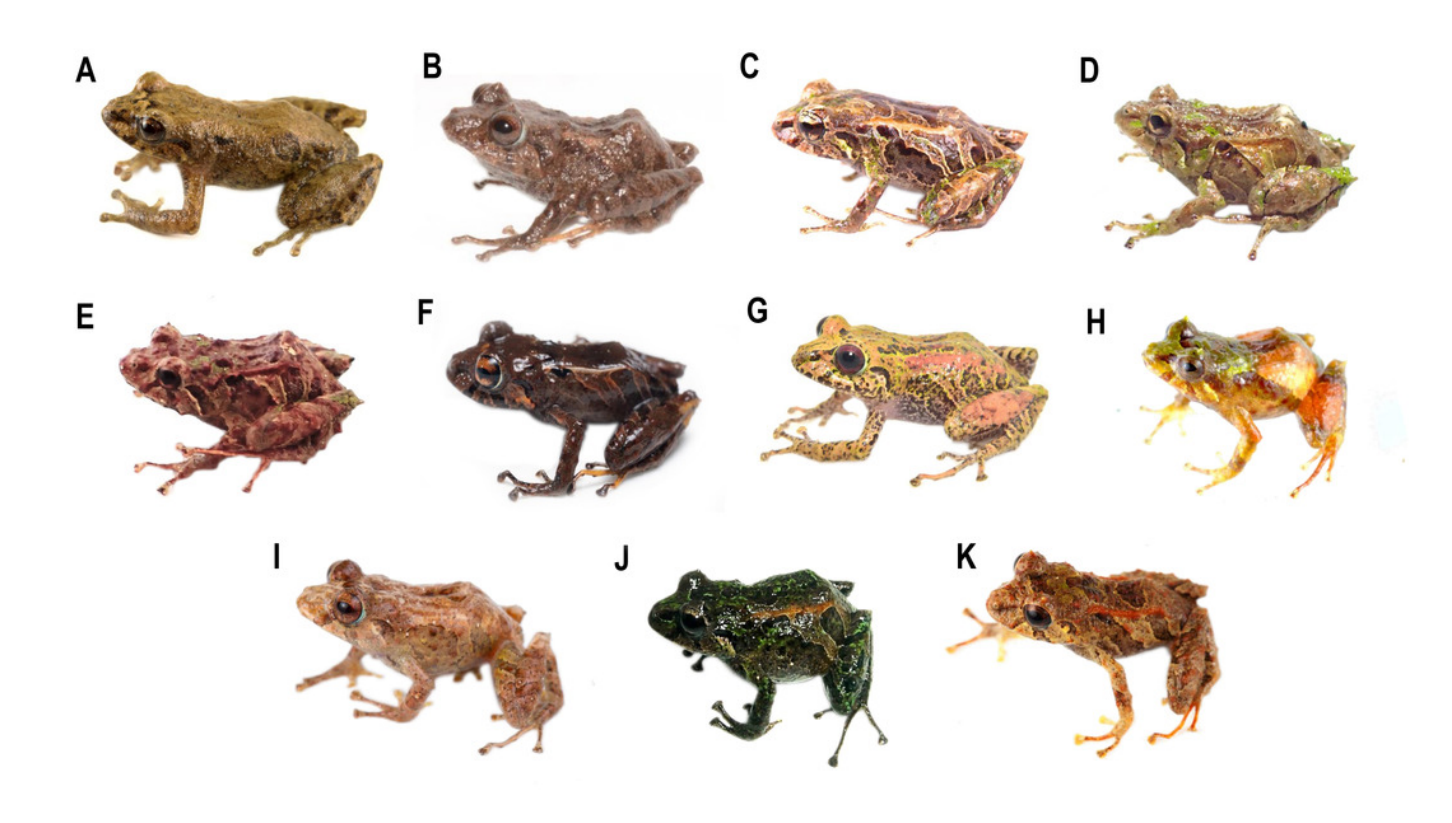




Figure 3.

Map of distribution of *Pristimantis celator* clade. Type localities are shown in red colors for different symbols. Dots with different colorations correspond to candidate species. Symbology for the formalin species described is indicated in the map legend.



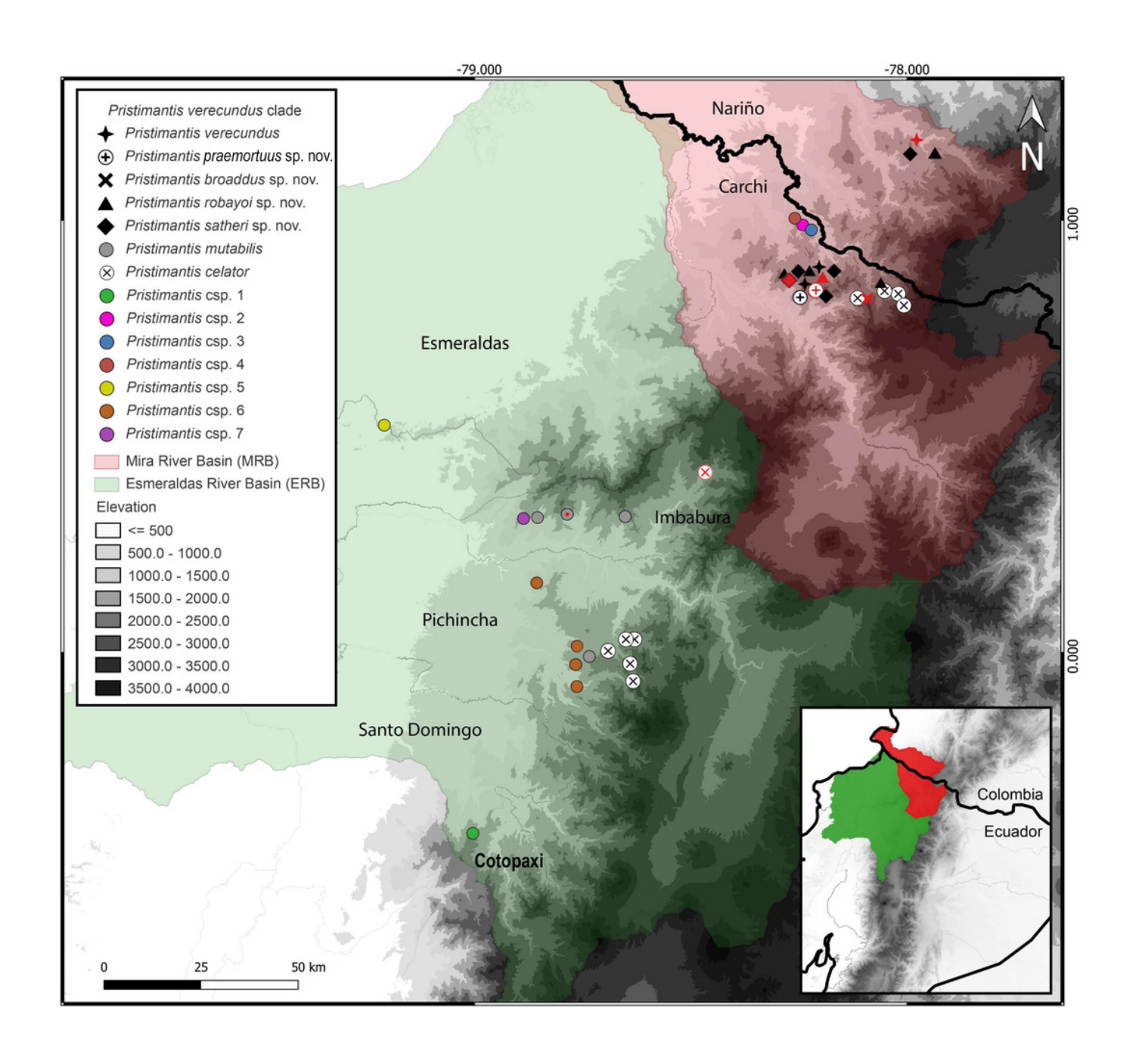
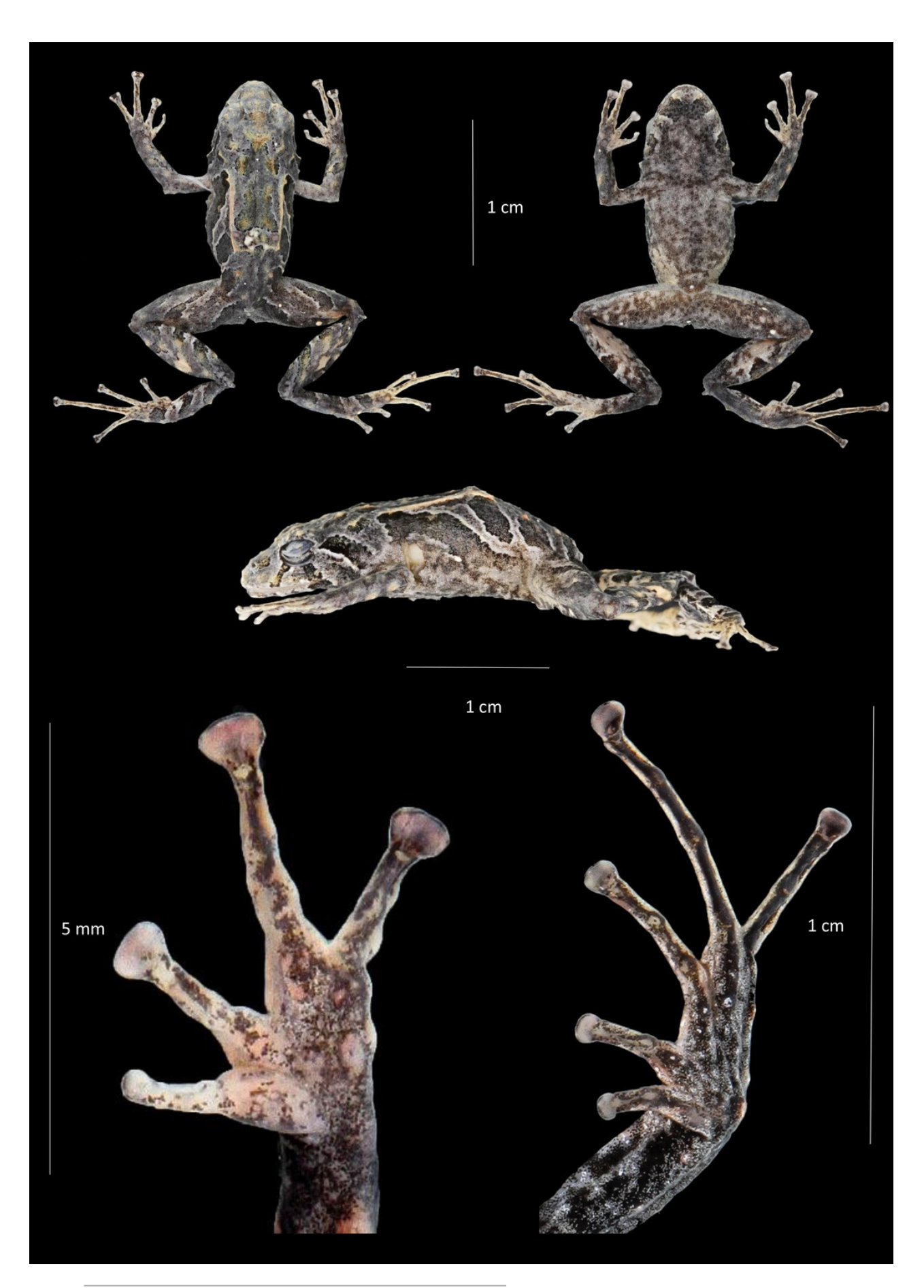




Figure 4

Dorsal, ventral and profile views of *Pristimantis praemortuus* sp. nov., (Holotype DHMECN 19591, female adult) and detail of hand and foot. Photographs Christian Paucar V.



PeerJ reviewing PDF | (2024:09:106009:0:1:NEW 16 Sep 2024)

Figure 5.

Comparison of heads in dorsal view of preserved of some species of *Pristimantis celator* clade. (A) *P. verecundus*, Holotype IAvH 1801; (B) *Pristimantis mutabilis*, DHMECN 11755; (C) *Pristimantis satheri* sp. nov., Holotype DHMECN 14858; (D) *Pristimantis robayoi* sp. nov., paratype, DHMECN 17894; (E) *Pristimantis praemortuus* sp. nov., Holotype, DHMECN 19591; (F) *Pristimantis broaddus* sp.nov., Holotype DHMECN 19037. Photographs Christian Paucar V.

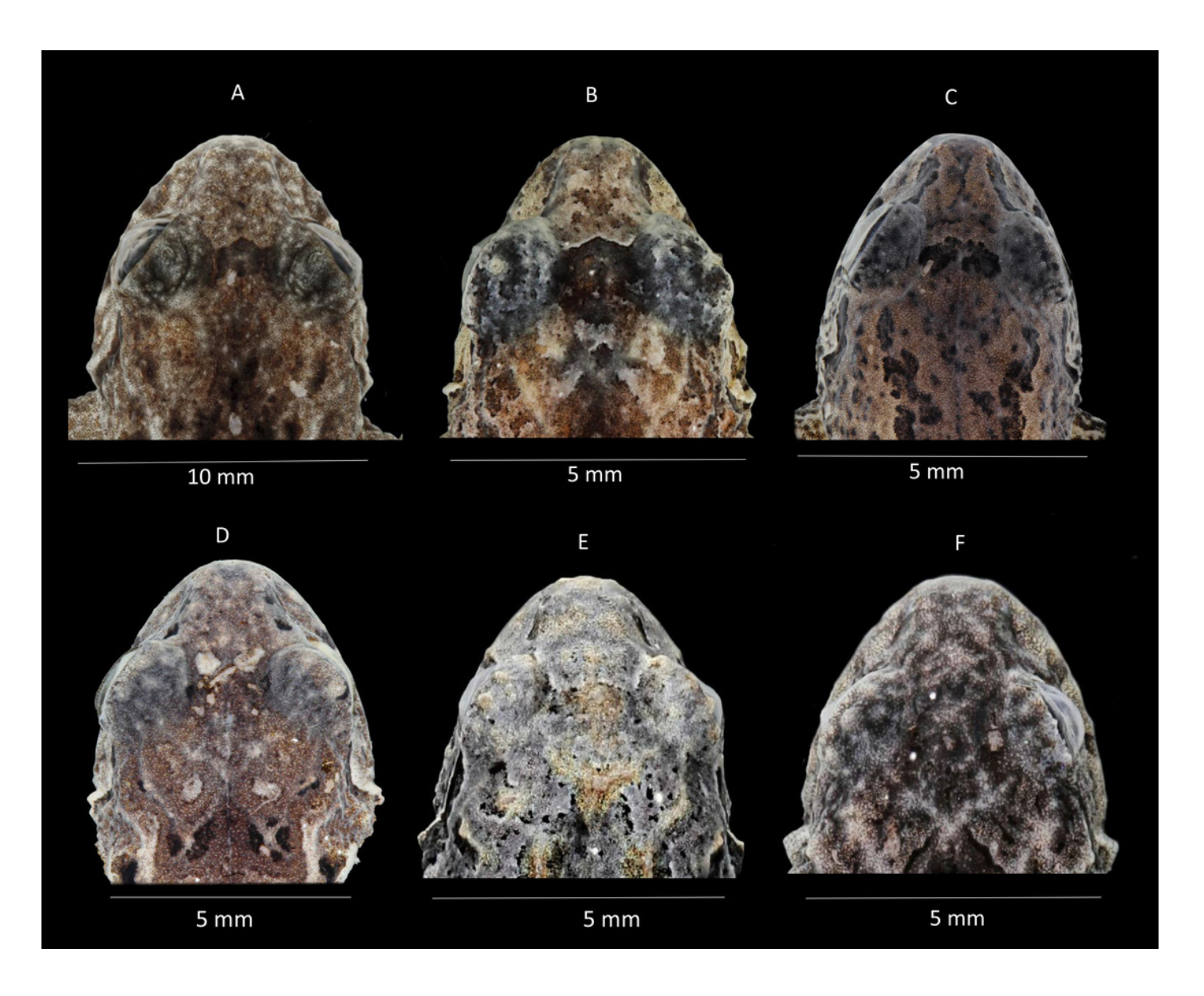


Figure 6.

Comparison of similar species of *Pristimantis celator* clade in life. (A) *P. verecundus* DHMECN 12599, male, SVL: 18.17 mm; (B) *P. satheri* sp. nov. DHMECN 14858, Holotype, female, SVL: 23.74 mm; (C) *P. robayoi* sp. nov., DHMECN 17984, Holotype, male, SVL: 24.22 mm; (D) *P. mutabilis*, QCAZ 76813; (E) *P. broaddus*, DHMECN 19029, female, SVL: 18.21 mm; (F) *P. praemortuus*, DHMECN 19591, female, SVL: 17.58 mm. Photographs by Mario H. Yánez Muñoz (A), Christian Paucar V. (E, F), Julio C. Carrión (C), Santiago R. Ron (D).

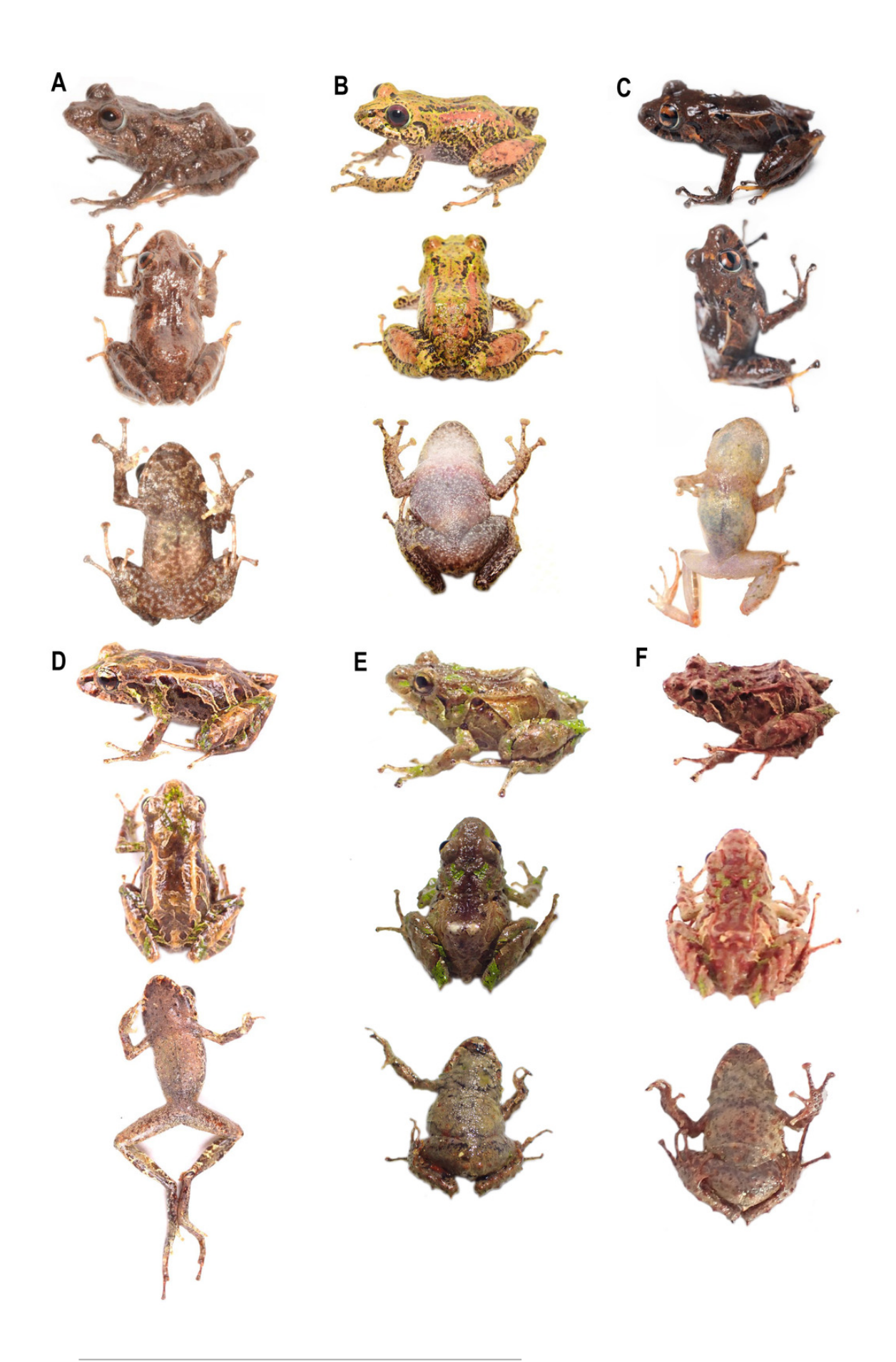


Figure 7.

Comparison of heads profiles views (A–B) and groin coloration (G–L) in life of similar species of *Pristimantis celator* clade. (A, G) *P. verecundus* DHMECN 17892; (B, H) *P. mutabilis*, no collected specimen; (C, I) *P. satheri* sp. nov. DHMECN 14858, Holotype, (D) *P. robayoi* sp. nov., DHMECN 17984, Holotype; (E, K) *P. broaddus*, DHMECN 19029; (F, L) *P. praemortuus*, DHMECN 19591. Photographs by Mario H. Yánez Muñoz (A), Christian Paucar V. (E, F, K, L), Julio C. Carrión (A, D), Santiago R. Ron (H), Jaime Culebras (G); Mateo Vega-Yánez (C, I).

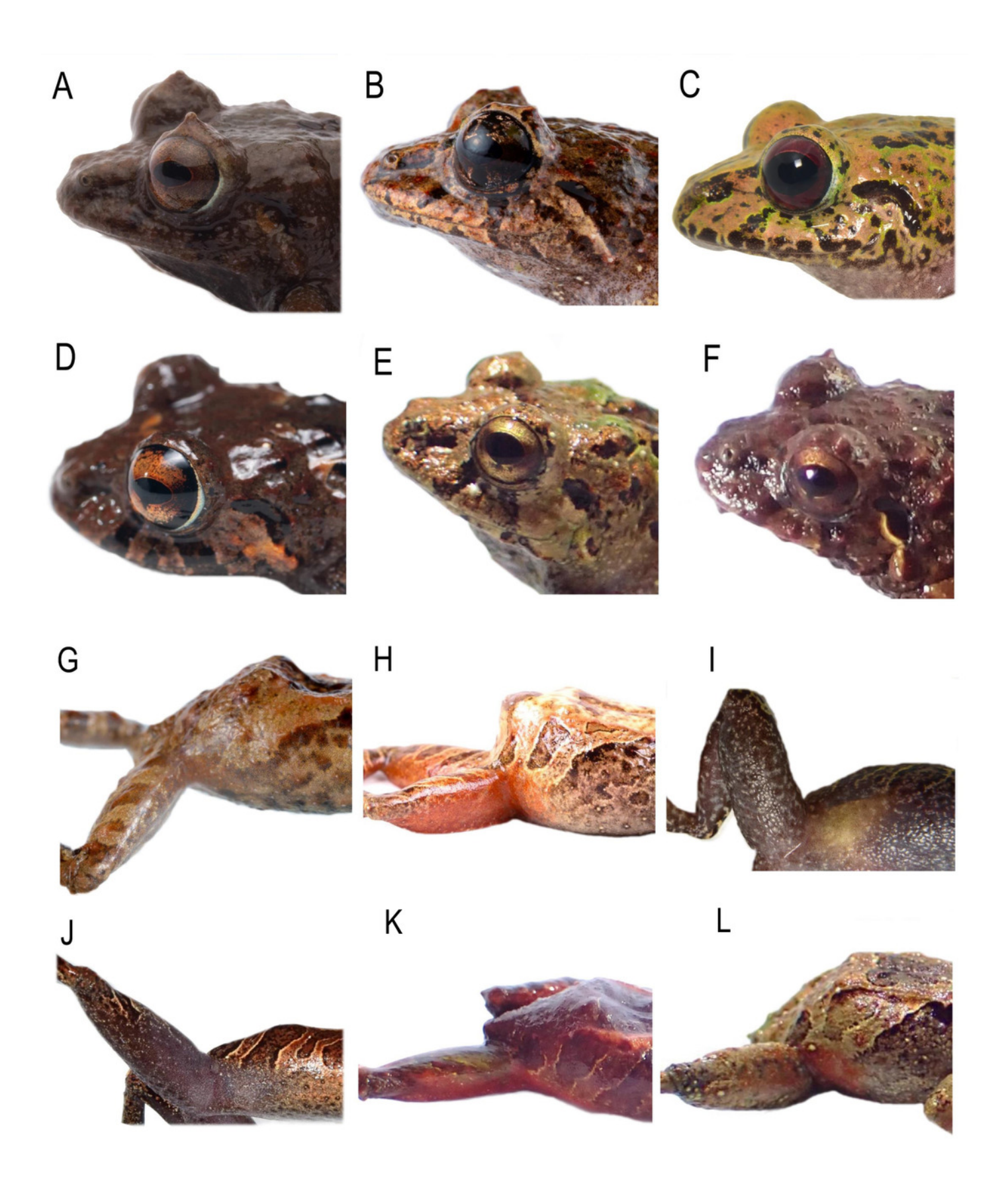




Figure 8.

Comparison in preservative of similar species of *Pristimantis celator* clade. (A) *Pristimantis verecundus*, Holotype IAvH 1801; (B) *Pristimantis mutabilis* DHMENC 11755; (C, G) *Pristimantis satheri* sp. nov., Holotype DHMECN 14858; (D, E) *Pristimantis robayoi* sp. nov., Holotype DHMECN 17894; (E) *Pristimantis praemortuus* sp. nov., Holotype DHMECN 19591; (F) *Prismtimantis boaddus* sp. nov., Holotype DHMENC 19037. Photographs Christian Paucar.

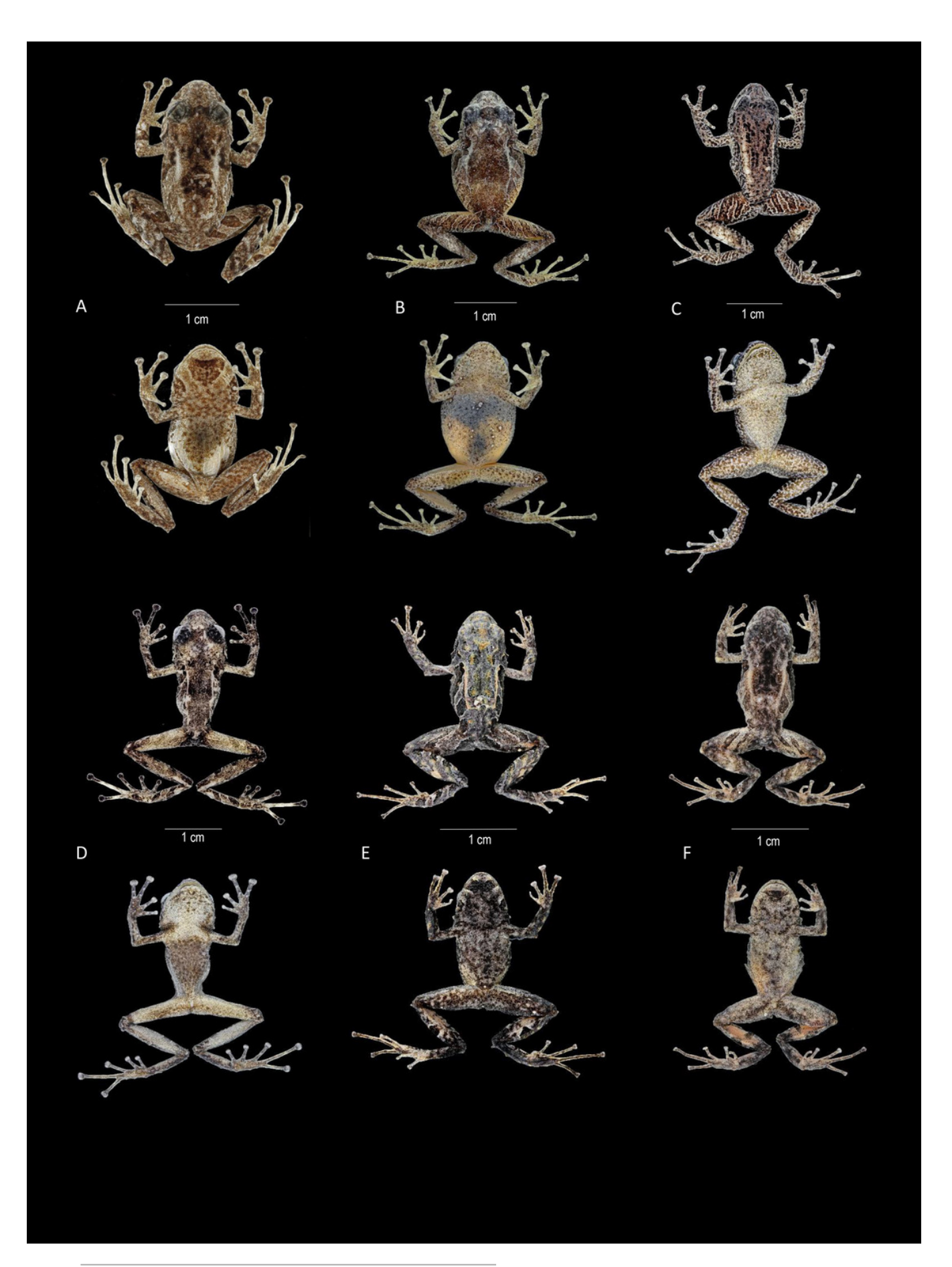




Figure 9.

Variation in life of the type series of *Pristimantis praemortuus* sp. nov. (A) DHMECN 19535, male, SVL: 16.39 mm; (B) DHMECN 19547, male, SVL: 14.76 mm; (C, G, K) DHMECN 19546, male, SVL: 12.46 mm; (D, H, L) DHMECN 19591, Holotype, female, SVL: 17.68 mm; (E, J, N). DHMECN 19557, female, SVL: 17.33 mm; (F, I, M) DHMECN 19570, female, SVL: 17.03 mm. Photographs by Christian Paucar.

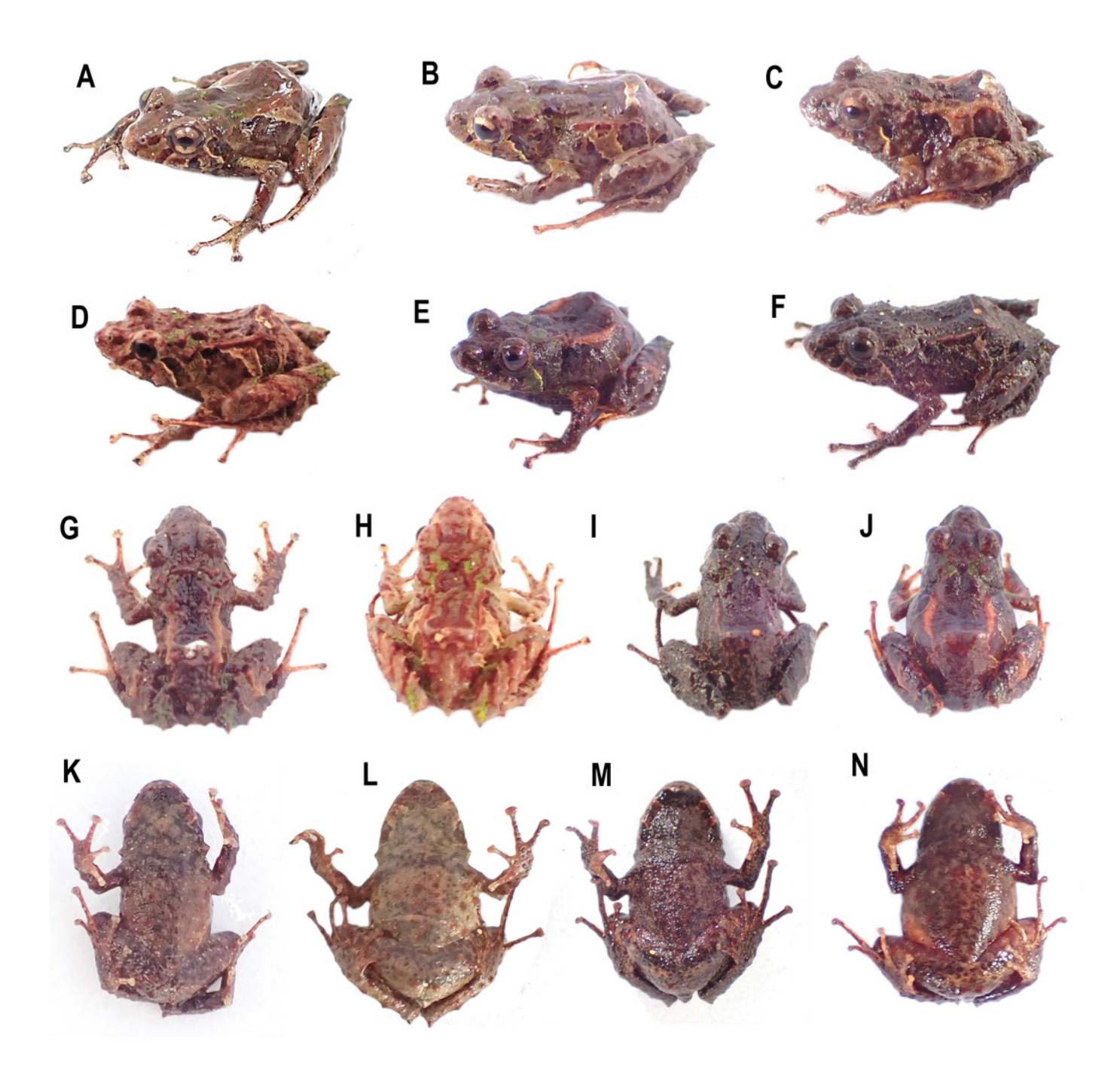




Figure 10.

Dorsal, ventral and profile views of *Pristimantis broaddus* sp. nov., female adult (DHMECN 19037) and detail of hand and foot. Photographs Christian Paucar V.



PeerJ reviewing PDF | (2024:09:106009:0:1:NEW 16 Sep 2024)



Figure 11.

Variation in life of the type series of *Pristimantis broaddus* sp. nov. (A) DHMECN 19029, female, SVL: 18.21 mm; (B, G, K) DHMECN 19037, Holotype, female, SVL: 18.21 mm; (C, H, L) DHMECN 19035, female, SVL: 17.49 mm; (D, I) DHMECN 19028, female, SVL: 16.81 mm; (E). DHMECN 19031, female, SVL: 17.57 mm; (F, J, M) DHMECN 19036, female, SVL: 16.55 mm. Photographs by Christian Paucar.

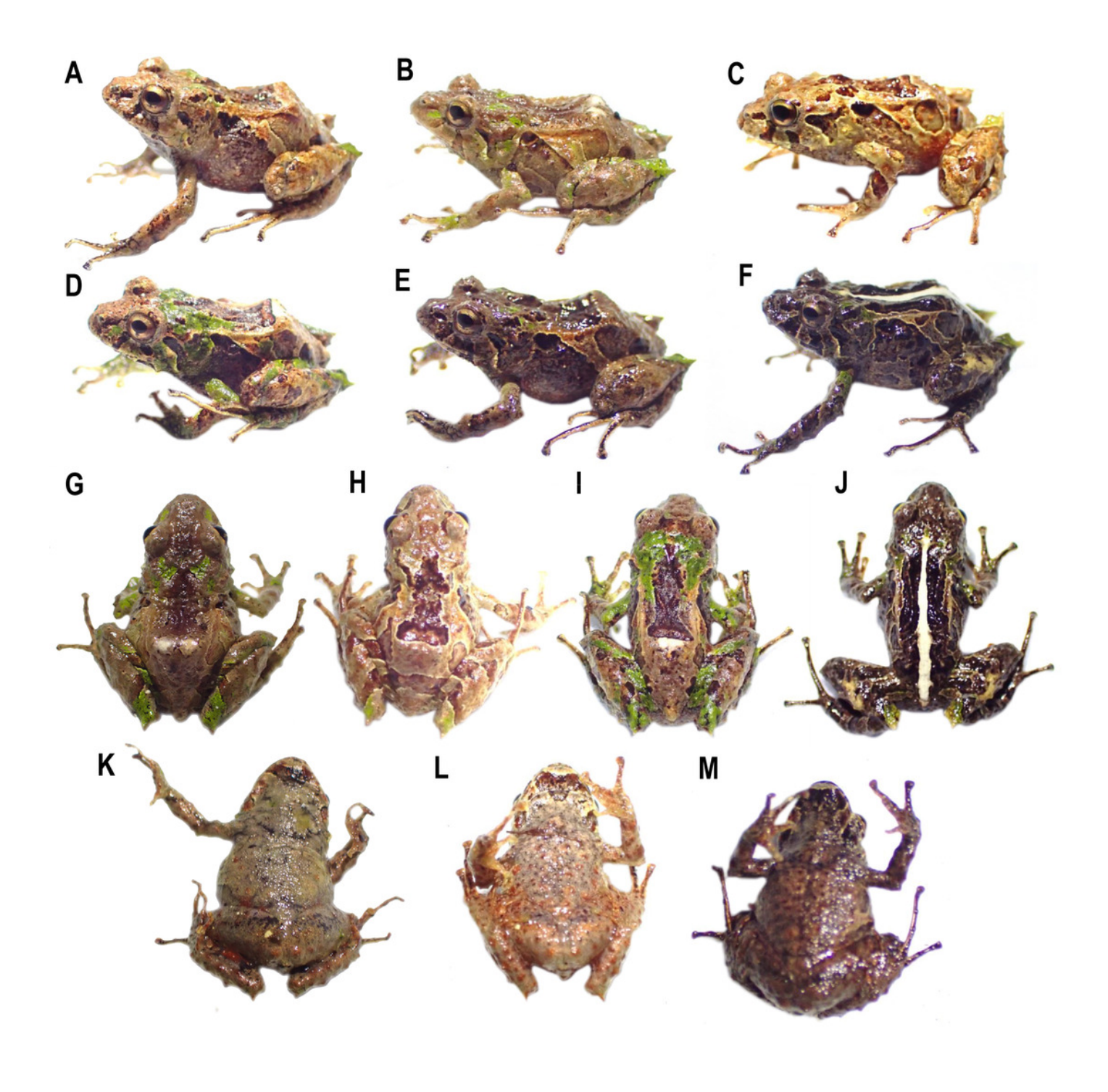
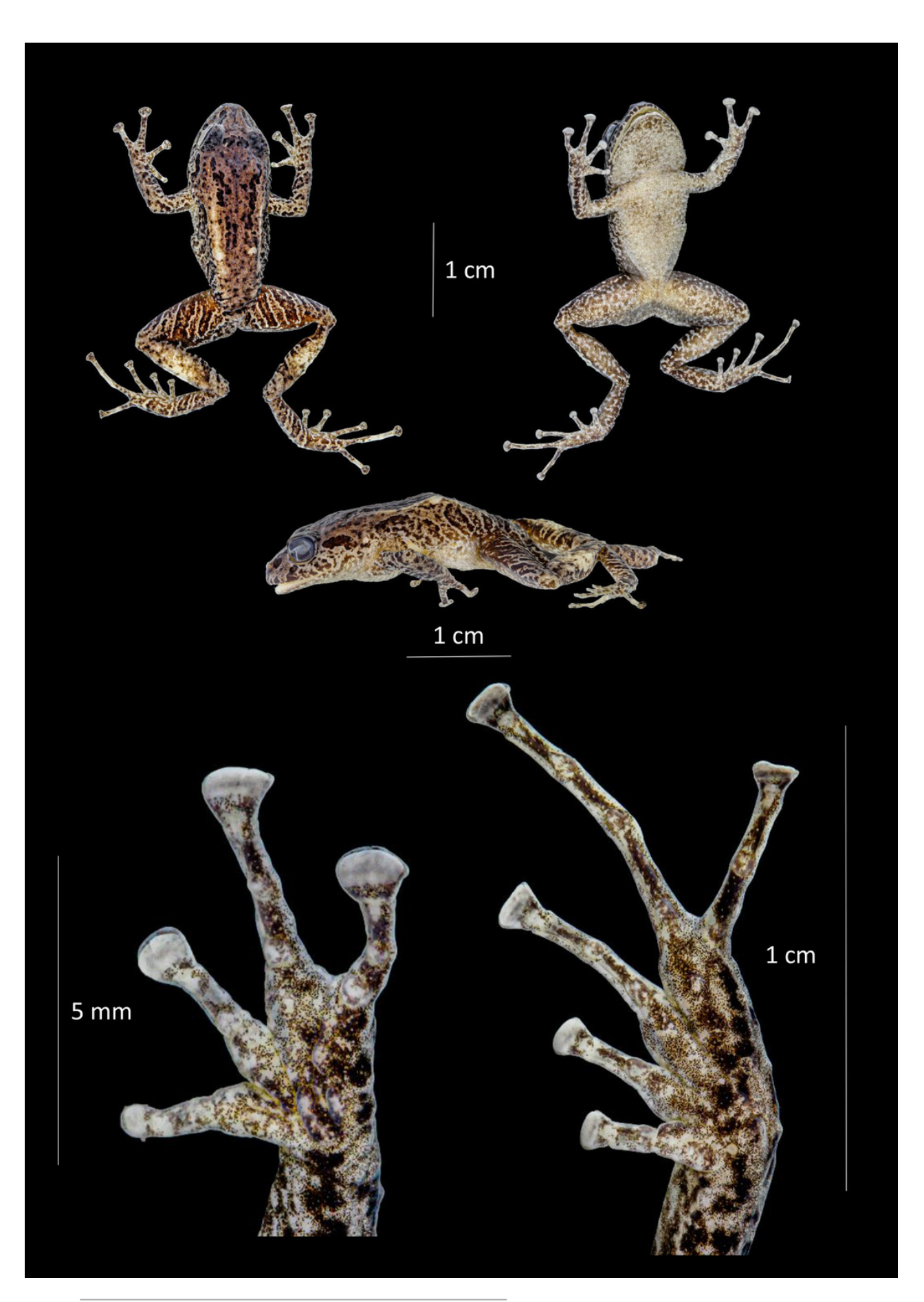




Figure 12.

Dorsal, ventral and profile views of *Pristimantis sathreri* sp. nov., female adult (DHMECN 14858) and detail of hand and foot. Photographs by Christian Paucar.



PeerJ reviewing PDF | (2024:09:106009:0:1:NEW 16 Sep 2024)



Figure 13.

Variation in life of the type series of *Pristimantis satheri* sp. nov. (A, E, H) DHMECN 14858, Holotype, female, SVL: 23.74 mm; (B, I) DHMECN 14885, female, SVL: 22.08 mm; (C, F, J) DHMECN 19538, male, SVL: 19.79 mm; (D, G) DHMECN I, juvenile, SVL: 14.71 mm. Photographs by Mateo Vega-Yánez (A, B, E, H, I), Julio C. Carrión-Olmedo (D, G), Christian Paucar (C, F, J).

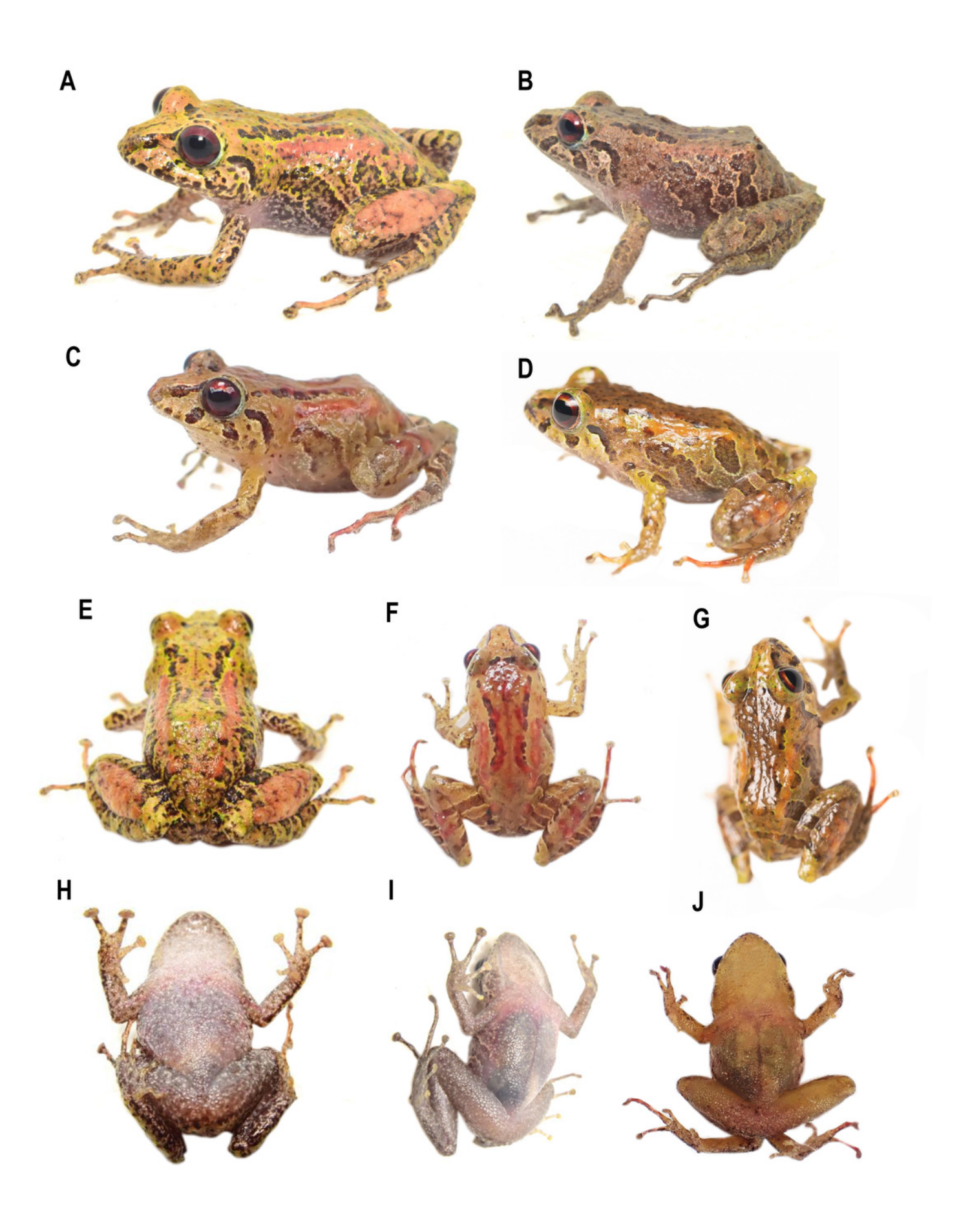
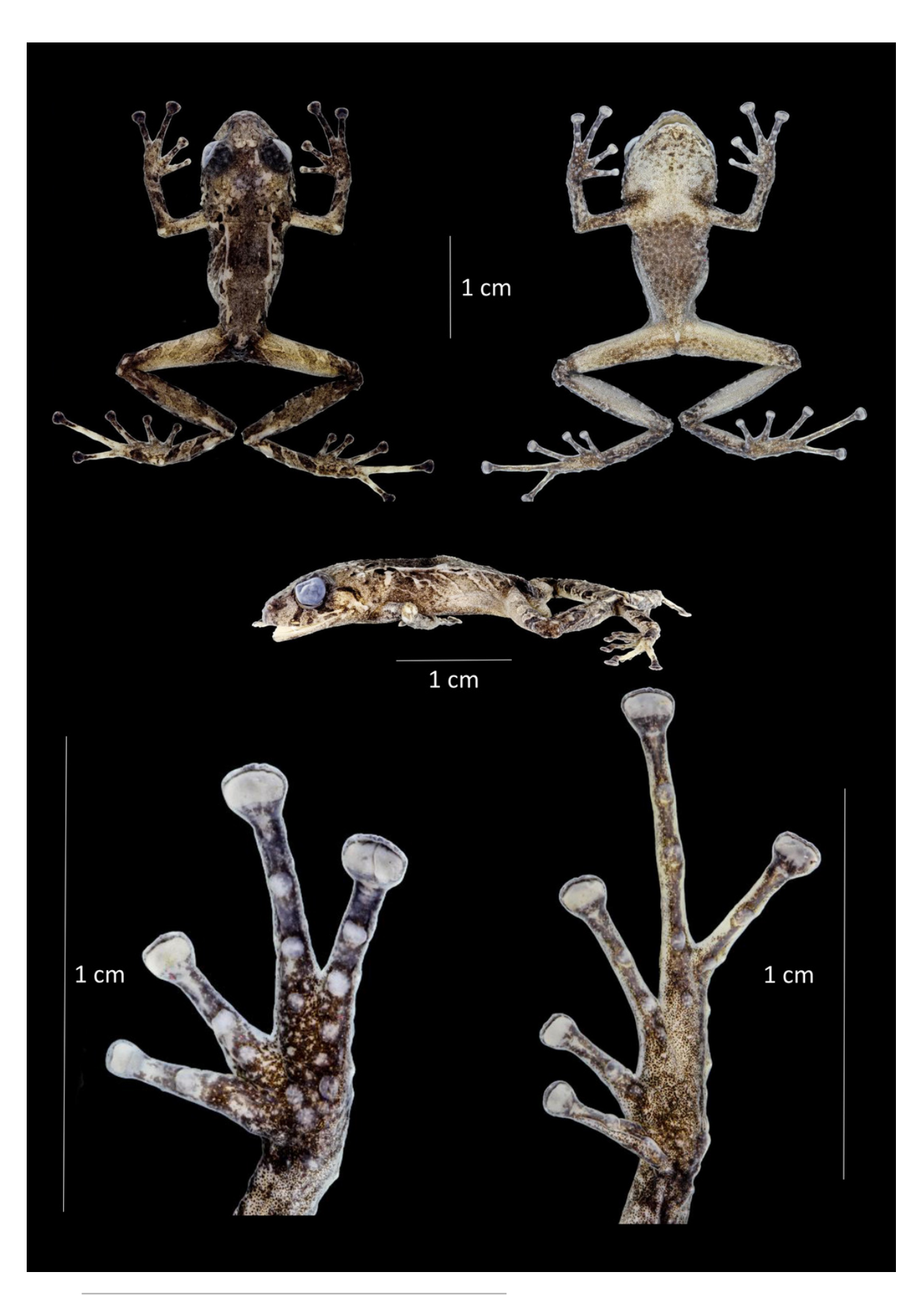




Figure 14.

Dorsal, ventral and profile views of *Pristimantis robayoi* sp. nov., male adult (DHMECN 17894) and detail of hand and foot. Photographs by Christian Paucar.



PeerJ reviewing PDF | (2024:09:106009:0:1:NEW 16 Sep 2024)



Figure 15.

Variation in life of the type series of *Pristimantis robayoi* sp. nov. (A) DHMECN 17894, holotype, male, SVL: 24.22 mm; (B, N) DHMECN 16150, female, SVL: 21.01 mm; (C, L) DHMECN 14884, female, SVL: 29.05 mm; (D, H, M) DHMECN 14885, male, SVL: 20.15 mm; (E) DHMECN 14953, juvenile, SVL: 20,15 mm; (F) DHMECN 14947, female, SVL: 25,83 mm; (G, K) DHMECN 14960, female, LRC: 27,96; (I) DHMECN 14950, juvenile, SVL: 18.16 mm; (J) DHMECN 14948, female, SVL: 25.18 mm. Photographs by Mateo Vega-Yánez (A, C-M, E, H, I), Juan P. Reyes-Puig (B, N).

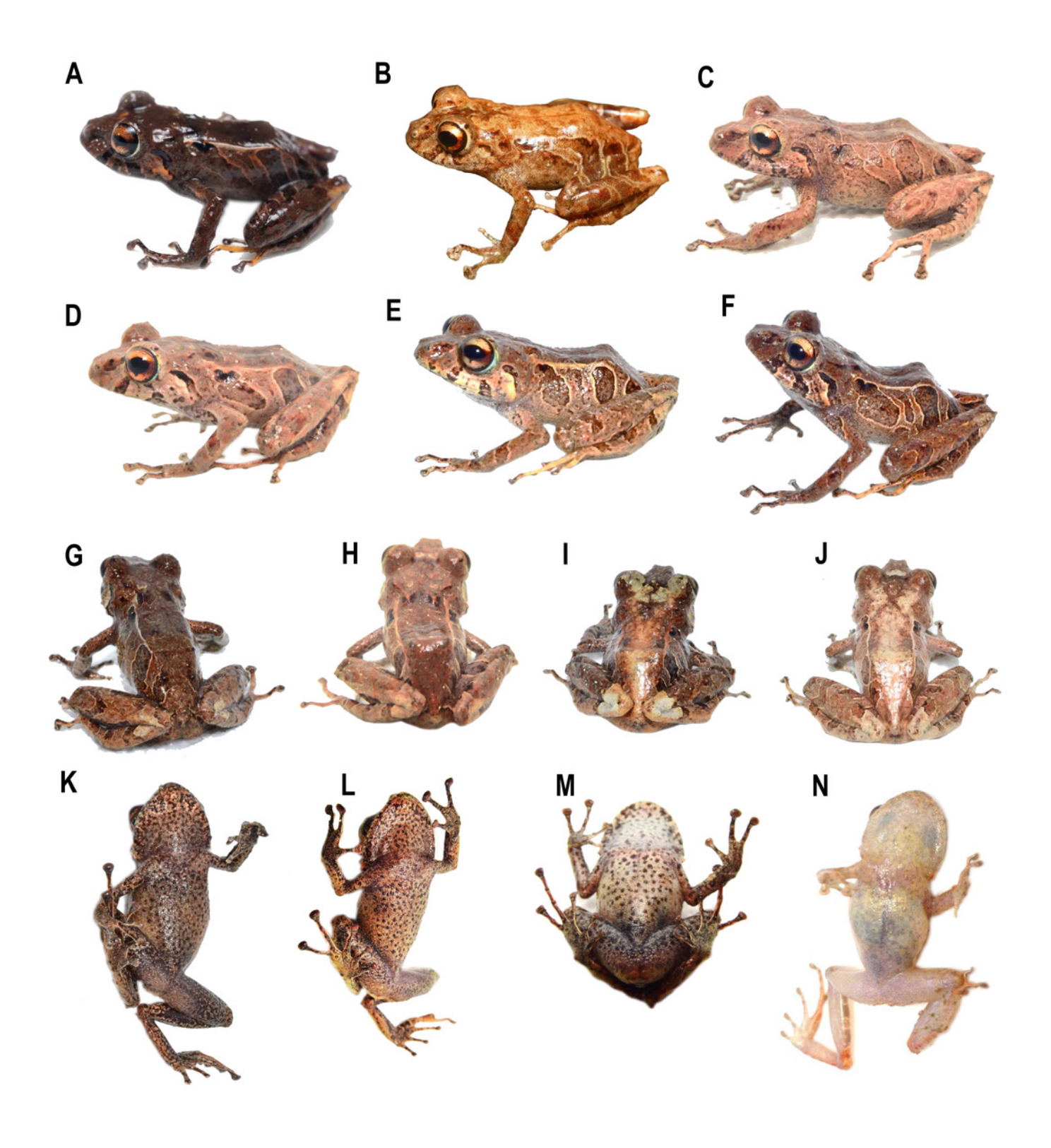


Figure 16.

Distribution and altitudinal range of *Pristimantis celator* clade. Symbols referred to in the legend of Figure 3. MRB= Mira River Basin, ERB= Esmeraldas River Basin. WMF= Western Montane Forest, WLMF= Western Low Montane Forest, WFOF= Western Foothill Forest Illustration by Mario H. Yánez-Muñoz.

